Phase equilibrium and dissociation enthalpies of CO2/cyclopentane hydrates in presence of salts for water treatment and CO2 capture: New experimental data and modeling

Angsar Serikkali, Hieu Ngo Van, Trung-Kien Pham, Quang Duyen Le, Jérome Douzet, Jean-Michel Herri, Baptiste Bouillot

Phase equilibrium and dissociation enthalpies of CO_2/cyclopentane hydrates in presence of salts for water treatment and CO_2 capture: new experimental data and modelling

Angsar Serikkali[1], Hieu Ngo Van[1, 2], Trung-Kien Pham[2], Quang Duyen Le[2], Jérôme Douzet[1], Jean-Michel Herri[1], Baptiste Bouillot[1]*

[1] *Mines Saint-Etienne, Univ Lyon, CNRS, UMR 5307 LGF, Centre SPIN, F - 42023 Saint-Etienne France;*

[2]*Oil Refinery and Petrochemistry Department, Hanoi University of Mining and Geology, Duc Thang, Bac Tu Liem, 100000 Hanoi, Viet Nam*

*Corresponding authors: bouillot@emse.fr

DOI : 10.1016/j.fluid.2022.113410

Abstract

The applications of clathrate hydrates on carbon dioxide capture and desalination is an attractive and growing subject within the hydrate community. While many promoters exists to overcome the numerous issues of hydrate-based technologies (mostly how to mild the operating conditions and improve the kinetics), there is a need to find a guest that could be recovered easily. That is why cyclopentane (CP), an organic molecule not miscible into water that can form hydrates under atmospheric pressure at 7°C, has been studied widely in the literature. However, its behavior in forming mixed hydrates with CO_2 in presence of salts is still not well understood. This work is an effort to investigate the thermodynamics of mixed CO_2/CP hydrates to fulfill the gap in this field from a thermodynamic point of view.

In this effort, new equilibrium data of mixed CO_2/CP hydrates in the presence of salts (NaCl-KCl, $MgCl_2$, $CaCl_2$ which are among the main factors of hard water) have been obtained under different concentrations and pressures. Final dissociation points and as well as intermediate metastable points were obtained.

Furthermore, thermodynamic consistency tests have been performed on our data and literature data to discuss their reliability. This test is important to question the idea of thermodynamic equilibrium since we suspect from a previous work the formation of several hydrate structures.

Finally, three modelling approaches were considered: van der Waals and Platteeuw (vdW-P) approach, Hu-Lee-Sum (HLS) correlation, and ice melting point method derived from HLS proposition.

Results showed a greater inhibition effect of cation Ca^{2+} compared to Mg^{2+} and that vdW-P method can predict equilibrium temperature within 0.2°C uncertainty.

Keywords: cyclopentane hydrates, hydrate-based desalination, carbon dioxide capture, hydrate dissociation enthalpy, thermodynamic consistency of hydrates

Introduction

This article aims at supporting the development of clathrate hydrate-based technologies for water treatment combined with CO_2 capture from a thermodynamic point of view.

Clathrate hydrates are ice-like crystalline solid compounds of guest and water molecules. The guest molecules are small non-polar molecules (typical gases like CO_2, CH_4, C_2H_6, etc.) or (non)polar molecules with large hydrophobic moieties such as cyclopentane (CP), Tetrahydrofuran (THF), etc which are trapped inside cages of hydrogen-bonded polyhedral [1,2]. Clathrate hydrates formation is not a chemical reaction. Under low temperature and high-pressure conditions, a first-order phase transition of water molecules occurs by constituting cavities through hydrogen-bonding networks. These cavities are thermodynamically unstable but stabilized by guest molecules' adsorption [2–4]. The phase equilibria of clathrate hydrates depend on the physical and chemical properties of the guest molecules. Additionally, the existence of additives in the system may vary the equilibrium conditions of clathrate hydrates.

For a long time clathrate hydrates were curiosity [5]. Flow assurance issue was probably one of the first significant hydrate study from and industrial point of view. Indeed, gas hydrate formation is the major cause of pipelines plugging in petroleum industries. Therefore, in the past, the focus of researching gas hydrates has been on preventing hydrate formation in pipelines. However, in the past two decades, clathrate hydrates have received much attention on their potential applications in many fields of industry [5] such as gas separation [6–12], gas storage and transportation (SNG, ANG, LNG, etc.) [13–21], CO_2 storage and capture (CCS) [22–29], cold storage and refrigeration [30–34], *etc*. Moreover, the huge reservoirs of natural gas hydrates in permafrost regions and marine sediments may provide a new source of sustainable energy [24,35,36]. Hassanpouryouzband *et al.* have deeply considered other applications in sustainable chemistry in a recent review [37].

The lack of fresh water is one of the biggest challenges people face [38]. The high level of salts and pollutants in water sources can be exacerbated by changes in precipitation patterns due to the climate crisis and an increase in the population in the region [39]. Therefore, desalination can assist with expanding the scope of accessible water assets and reach net-zero carbon emission by 2050 [40]. Many desalination technologies are being widely used and developed such as multi-stage flash distillation (MSF), membrane distillation, electro dialysis, forward osmosis, reverse osmosis, and so on. On top of that, Hydrate Based Desalination (HBD) is an application of gas hydrate that can be a novel candidate to solve the problem [41]. The idea is based on salt elimination. When gas hydrate forms in seawater, the salts are outside of the hydrate cages and stay in the concentrated

aqueous solution that can be removed by a physical process [37]. There are interesting developments in HBD process [4,42–46] up to 80% efficiency [47], but HBD requires in-depth research in term of the effectiveness and safety. The development is the combination of desalination with carbon capture, using CO_2 as a guest for hydrate formation. Hereafter, one of the potential use of the stored CO_2 is to come forward as the working fluid to boost the geothermal energy development [27–29]. The second is the use of appropriate thermodynamic promoters to enhance hydrate formation.

Hydrates promoters are widely investigated in the hydrate-based process developments due to their capabilities of improving hydrate formation rate and moderate the equilibrium pressure. Tetrahydrofuran (THF) and tetra-butyl ammonium salts (such as TBAB, TBAC and *etc*.) are among the most discussed types of additives [48–55]. Despite their advantages in increasing the salt removal efficiency, their solubility in water is a major issue. Recently, cyclopentane (CP) has been recognized as being an interesting promoter since it enhances the hydrate formation conditions and is immiscible with water [41,56]. Therefore CP is one of the few promoters that can be recovered after dissociation except from gaseous promoters. In the end, many efforts can be found on CP hydrates in presence of salts, but only a few for mixed CO_2/CP hydrates. Let's mention the work of Zheng et al.[57], Hong et al. [46] and Lee et al. [58] in presence of NaCl and previous effort of Maghsoodloo Babakhani et al. [45] in presence of both NaCl and KCl.

Nevertheless, there is still a need for more phase equilibrium data of mixed CP-CO_2 hydrates in order to improve and develop hydrate-based carbon capture and desalination. Hence, in this work, four-phase equilibrium data (V-L_w-L_{HC}-H) for CP-CO_2 binary hydrates in the presence of diverse salts ($MgCl_2$, $CaCl_2$ in particular, which are the main factor causing hard water), but also mixtures of NaCl and KCl) solutions have been investigated. The experiments have been carried out in a batch reactor and by an isochoric technique. Moreover, concentrations of salts at intermediate metastable and total dissociation states have been analyzed. The experimental results were then discussed and compared to the literature.

At the same time, thermodynamic consistency and modelling have been investigated on these and literature results. First of all, simple clapeyron's equation has been considered. Then, Sa et al. [59] consistency test has been employed. This first step, in addition to discussing thermodynamic consistency, is also a way to calculating dissociation enthalpies. In order to enlarge the scope of this study and compare our results to other similar systems, literature data for mixed methane/CP hydrates in presence of NaCl have been considered [60].

Then thermodynamic modelling has been performed to predict equilibrium temperatures according to three different approaches: standard van der Waals and Platteeuw (vdW-P) [59], HLS correlation [60,69,70], and new method derived from HLS correlation taking as reference the ice suppression temperature [61].

Finally, some conclusions and comments on possible future work finish this article.

2. Experimental section

2.1. Materials

All materials used in this work are listed in detail in **Table 1.** Ultrapure water was provided by the Milli-Q®-Advantage A10 water purification system. It produces water with conductivity less than 0.055 $\mu S.cm^{-1}$ and TOC (total organic carbon content) less than 5 ppb.

Table 1. Materials

Name	Purity	Supplier
Cyclopentane	98%	Sigma Aldrich
Sodium Chloride	99.5%	Sigma Aldrich
Potassium Chloride	99%	Sigma Aldrich
Magnesium Chloride	98%	Sigma Aldrich
Calcium chloride dihydrate	99%	Sigma Aldrich
Carbon dioxide	99.999%	Air Products

2.2. Experimental set-up

The Experimental set-up is similar to previous efforts [45]. A schematic of the experimental setup is shown in **Figure 1**.

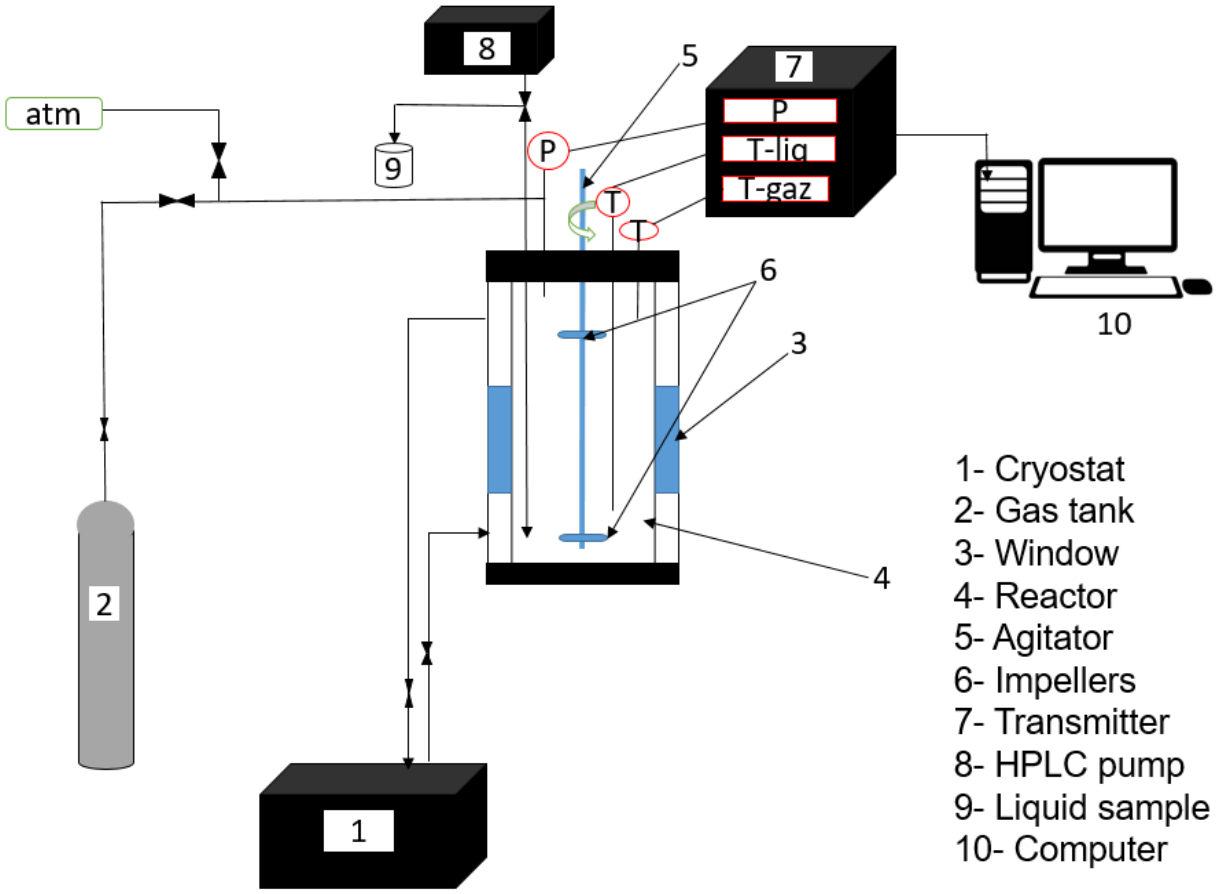

Figure 1. The schematic of the experimental set-up

Two same characteristics batch reactors (with the inner volume, the first is 2.36 liter and the second 2.23 liter) were developed and used to study the phase equilibria of clathrate hydrates as well as kinetics. Both are equipped with transparent windows that allowed direct observation. Each reactor is covered by an isolation jacket and the inner temperature is controlled by a cryostat LAUDA RC6 CS ranging from -15 to 50°C. There are vertical agitators with two sets of blades; the top set is in the gas phase and the bottom one is in liquid. The temperatures inside the reactor including gas and liquid phase's temperature are determined by two Pt100 temperature sensors at the top and bottom of the cell, respectively. The accuracy of these probes is ±0.2 C. The pressure is also measured by a pressure probe in the range 0-10 MPa with the accuracy of ±0.01 MPa. Water, solution, and CP can be injected into the reactors by a KNAUER P4.1S HPLC pump at high pressure. The working rate of the pump is between 0.1 and 50 ml/min at the pressure up to 10Mpa. A mechanical valve is connected to a capillary tube in the liquid phase to take liquid samples during the experiments. Data acquisition is controlled on a personal computer running Labview. The samples are then analyzed by ion chromatography system Dionex ICS-5000^{+}.

2.3. Experimental procedure

After cleaning the autoclave with pure water, the air and other impurities are removed by using a vacuum pump for 40 minutes. The reactor is then filled with CO_2 at the desired pressure. The pressure is monitored at a stable temperature for 24 hours to ensure that there is no gas leak in our experimental setup. The ultrapure water is used to prepare the salt solution at chosen concentration right before injecting into the reactors. Thanks to the HPLC pump, about 400 mL of prepared solution and 43.9 mL cyclopentane are introduced to the cell (volumetric ratio between the aqueous solution and cyclopentane is about 9:1). The temperature is then decreased to 1°C. After several hours for the gas dissolution into the liquid phase and the induction time, crystallization starts. As result of hydrate formation, the temperature slightly increases in a short term. From this point, it is necessary to wait for 2-3 days to attain equilibrium with no change in temperature and pressure. That is depended on the initial concentration of aqueous solution as well as pressure. Once the equilibrium is reached, about 1-2 mL of the liquid sample is taken to measure the salt concentration by ionic chromatography. Then, the dissociation process is started by stepwise temperature increasing (1 °C/h) and we wait for the stability of pressure and temperature. A liquid sample is taken at several metastable equilibrium points. At 2°C below the final equilibrium point, the temperature is augmented 0.3-0.5 °C/h until the total dissociation. A liquid sample is taken at final equilibrium (total dissociation of hydrates). The temperature is increased to reach the initial condition. The initial pressure is then changed by purging or inserting CO_2 and the procedure is repeated to obtain further equilibrium points.

Note that all experimental uncertainties have been determined and presented before Herri et al. [3] and Son et al. [61].

2.4 Studies systems

Table 2 provides all initial conditions that have been considered.

Table 2. Initial conditions for experiments

No	NaCl (wt%)	KCl (wt%)	$MgCl_2$ (wt%)	$CaCl_2$ (wt%)	$m_{solution}$ (g)	m_{CP} (g)	V_R (L)	T_0(K)	P_0(bar)
±0.002wt%	±0.002wt%	±0.002wt%	±0.002wt%	±0.002wt%	±0.01 g	±0.01g	±0.01 L	±0.2K	±0.1 bar
1	1.75	1.75	0	0	400.23	33.39	2.36	291.0	24.9
2	1.75	1.75	0	0	399.08	33.21	2.36	292.5	20.3
3	1.75	1.75	0	0	398.07	33.05	2.36	291.3	16.4
4	1.75	1.75	0	0	398.23	32.98	2.36	290.6	10.5
5	0	0	3.5	0	404.84	33.36	2.23	290.5	21.5
6	0	0	3.5	0	400.4	33	2.23	292.9	25
7	0	0	3.5	0	393.48	32	2.23	292.8	23.1
8	0	0	5	0	500.49	41	2.36.	294.2	25
9	0	0	5	0	400.5	33	2.36	295.6	25.3
10	0	0	5	0	395.82	33	2.36	291.8	20
11	0	0	7	0	401	32	2.23	293	24.6
12	0	0	7	0	395.16	32	2.23	292.1	20.2
13	0	0	7	0	388.6	32	2.23	293.4	17.5
14	0	0	10	0	420	33	2.36	294	26.8
15	0	0	10	0	415.57	33	2.36	291.6	21.8
16	0	0	10	0	410	33	2.36	291.6	18.7
17	0	0	0	4	404	33	2.23	289.4	23
18	0	0	0	4	398	33	2.23	291.6	20.1
19	0	0	0	5	434	34	2.36	289	25.1
20	0	0	0	5	418.8	34	2.36	291.5	22.9
21	0	0	0	7	400.9	33.14	2.23	293.1	24
22	0	0	0	7	399.73	33.06	2.23	292	20.2
23	0	0	0	7	398.5	32.98	2.23	293.3	16
24	0	0	0	10	400.21	33.37	2.23	295.1	25.4
25	0	0	0	10	399.8	33.2	2.23	293.2	20.2
26	0	0	0	10	398.56	33.12	2.23	293	16

3. Thermodynamic consistency and calculation

3.1 The Clausius-Clapeyron

Enthalpy of dissociated hydrates is generally acquired by direct measurements like calorimetry (DSC) [62] or indirect calculation by the Clausius-Clapeyron equation [63]. MD simulation can

also be performed to determine dissociation enthalpies with quite good agreement with the methods mentioned above [64,65], especially under 304 K [66]. The hydrate formation and dissociation can be described by the following reaction:

$$CO_2 + aCP + bH_2O \leftrightarrow CO_2 \cdot aCP \cdot bH_2O \quad (1)$$

where *a* and *b* are known as mole numbers of CP and H_2O in hydrate, respectively.

The molar hydrate dissociation enthalpy change $\Delta_{\mathrm{diss}}H_{\mathrm{m}(CO_2)}$ is estimated through the slope between ln(P) and 1/T by the Clausius-Clapeyron equation [63]:

$$\frac{d\ln(P)}{d(1/T)} = \frac{-\Delta_{\mathrm{diss}}H_{\mathrm{m}(CO_2)}}{ZR} \quad (2)$$

In this case, *P* is the pressure, *T* is the temperature, $\Delta_{\mathrm{diss}}H_{\mathrm{m}(CO_2)}$ is the molar dissociation enthalpy of CO_2, R is the universal gas constant and Z is the compressibility factor of CO_2 at each equilibrium point, which is can be calculated by the Soave-Redlich-Kwong (SRK) equation of state [67]. Note that only CO_2 is considered in the gas phase so that CP and water presence is neglected and there is no need for a more complex equation of state.

According to Clapeyron's equation, the slope of ln(P) and 1/T should be linear, providing that the dissociation enthalpy and Z do not change significantly in the usual narrow range of temperature (0°C to 20°C). Therefore, Eq. (2) can be utilized to estimate $\Delta_{\mathrm{diss}}H_{\mathrm{m}(CO_2)}$. Nonetheless, note that Clapeyron's equation is relevant for a given system composition. If the hydrate composition changes, so does the dissociation enthalpy.

Finally, the linearity of Eq. (2) provides an estimation of the thermodynamic consistency of a given dataset. This test is indeed the first considered by Sa et al. [59] in their interesting work suggesting three assessments to account for thermodynamic consistency. These will be detailed in the next section.

3.2 Thermodynamic consistency

Based on the relatively constant relation of dissociation enthalpy and compressibility factor in Eq. (2), Sa et al. [59] demonstrated three assessment tests for thermodynamic consistency. They are described below with the evaluation range for each assessment in **Table 3**:

Assessment 1: For each salt concentration, the slope between ln(P) and 1/T presents a linear regression and gives R^2,%, which is depicted as 1-R^2,%. This assessment comes from the independence of $\Delta_{\mathrm{diss}}H/Z$ with water activity.

Assessment 2: The slope of regressed curves (with thermodynamic inhibitors (THI)/salts A_{THI}) in comparison with the slope for pure water (W) gives a relative deviation $(A_{THI}-A_W)/A_W \times 100$,%.

Assessment 3: This final assessment is related to the relative standard deviation (RSD),% of $\Delta T/T_0T$ which comes from the constant ratio $n / \Delta_{\text{diss}}H_{\text{m}(CO_2)}$ (the hydration number over the dissociation enthalpy) assuming a constant water activity for a given salt concentration. It can be described by the following equation:

$$\frac{\Delta T}{T_0 T} = -\frac{nR}{\Delta_{\text{diss}}H_{\text{m}(CO_2)}} \ln a_w \tag{3}$$

where T_0 and T phase equilibrium temperatures for pure water and inhibited system, respectively.

Table 3. Evaluation criteria for each assessment test.

	Assessment 1	Assessment 2	Assessment 3
Range	pass<2,5%	pass<±5%	pass<5%
	acceptable = 2,5-5%	acceptable ±5-10%	acceptable 5-10%
	5%<fail	±10%<fail	10%<fail

In our effort, new experimental data, as well as literature data, are discussed according to Sa et al. test.

4. Modelling thermodynamic equilibrium of mixed CP/CO_2 hydrates

Before presenting experimental results, the different thermodynamic models used to reproduced experimental equilibrium temperatures will be shortly detailed. Three approaches have been considered: van der Waals et Platteeuw (vdW-P) model [68], Hu-Lee-Sum (HLS) correlation [69], and Sa and Sum [70] method based on ice suppression temperature. To compare experimental results to models, the Absolute Average Deviation (AAD) will be used:

$$AAD = \frac{1}{N}\sum_{i=1}^{N\Sigma}\left|T_{i,pred} - T_{i,exp}\right| \tag{5}$$

where N is the number of experimental data points, Ti, pred (K) is the predicted equilibrium temperature, and Ti,exp (K) is the experimental equilibrium temperature.

4.1 vdW-P

The van der Waals and Platteeuw (vdW-P) model [68] can be employed to describe the clathrate hydrate phase equilibrium. This thermodynamic model has been described in detail in previous work [45,71,72]. However, here are some fundamental principles for the liquid/hydrate equilibrium.

Just note that, in this work, the CO_2 Kihara parameters were taken from Herri et al [71]. CP parameters were optimized by Maghsoodloo Babakhani et al. [45] based on the data in pure water

from Wang et al [73], data from NaCl solution by Zhang et al [74], and theirs. PHREEQC was used to provide water activity in brine solutions (pitzer database). The others parameters have been taken from the literature (Herri et al.[71] and Ho-Van et al.[61]).

Finally, note that the SRK equation of state was used for the CP/CO_2 vapor-liquid equilibrium and fugacities. The presence of water in the vapor and CP phase were neglected. The solubility of CO_2 in water was calculated based on the method described by Galfré [75]. The details of Kihara parameters for CP and CO_2 are presented in **Table 4**.

Table 4. Kihara potential parameters

Guest molecule	*a*	ε/κ	σ	Reference
CP	0.8968	262.318	2.641	[45]
CO_2	0.6805	168.77	2.963	[76]

4.2 HLS correlation

Hu-Lee-Sum (HLS) correlation was proposed by Hu et al. [69,77,78], and based on the fundamental principle of freezing point depression, they represented a new correlation for mixed clathrate hydrates. At first, the correlation has been developed for hydrates with the structure I in presence of single inhibitors (salts) [78], and hereafter they modified it to the systems with mixed salts and structure II hydrates [69]. On the one hand, they reported that the ratio of hydration number and enthalpy change $nR\ /\ \Delta_{\mathrm{diss}}H$ in Eq. (6) is considered as a function of pressure and suggested as constant. Hu et al. concluded $nR\ /\ \Delta_{\mathrm{diss}}H{=}\beta_1$, to express the structure I.

$$\frac{\Delta T}{T_0 T} = -\frac{nR}{\Delta_{\mathrm{diss}}H}\ln a_w = -\beta_1 \ln a_w \tag{6}$$

On the other hand, they concluded that $\ln a_w$ is only dependant on the effective mole fraction X, therefore constant at a given salt concentration. The relationship between $\ln a_w$ and X is the so-called HLS correlation:

$$\frac{\Delta T}{T_0 T} = -\frac{nR}{\Delta_{\mathrm{diss}}H}\ln a_w = C_1 X + C_2 X^2 + C_3 X^3 \tag{7}$$

Furthermore, they provide an extension of Eq. (6) in Eq. (8) to describe structure II hydrates and the ratio of $\Delta T/T_0 T$ for structure II and I corresponds to $\beta_2/\beta_1 = \alpha$.

$$\frac{\left(\frac{\Delta T}{T_0 T}\right)_2}{\left(\frac{\Delta T}{T_0 T}\right)_1} = \frac{R\ln a_w\left(\frac{n}{\Delta_{\mathrm{diss}}H}\right)_2}{R\ln a_w\left(\frac{n}{\Delta_{\mathrm{diss}}H}\right)_1} = \frac{\beta_2}{\beta_1} = \alpha \tag{8}$$

where 1 and 2 subscripts represent structure I and II, respectively, n is a hydration number and a_w refers to water activity. In our case, we consider CO_2-CP hydrate in presence of salts, we expect to have CO_2 hydrate in form of structure I and CP-CO_2 hydrate for structure II.

After α is found, the suppression temperature for hydrates with structure II can be predicted by HLS correlation:

$$\left(\frac{\Delta T}{T_0 T}\right)_2 = \alpha \times \left(\frac{\Delta T}{T_0 T}\right)_1 = \alpha \times (C_1 X + C_2 X^2 + C_3 X^3) \tag{9}$$

So that:

$$T = T_0 \times \left[1 + \alpha \times \left(\frac{\Delta T}{T_0 T}\right)_1\right]^{-1} \tag{10}$$

where C_1, C_2 and C_3 are fitting coefficients which are taken from the first paper of Hu et al. [78]. X is the effective mole fraction and can be found and given by:

$$X = \Sigma_{j=salts} = \Sigma_{i=ions} = \left|z_{jj i}\right| x_{jj i} \tag{11}$$

where z and x correspond to ion charge number and mole fraction, respectively.

4.3 Ice melting point method (HLS proposition)

Recently, Sa et Sum, have drawn our attention to their newest paper and correlation by ice melting point method [70]. Since the presence of inhibitors in the hydrate system, lowers water activity and changes the phase equilibrium temperature as in freshwater, they propose to predict the suppression temperature of hydrates through suppression temperature of water freezing point. This approach is somehow similar to HLS correlation, except that pure ice is considered instead of the structure I hydrates. Therefore, they modified Eq. (6) as follows:

$$\left(\frac{\Delta T}{T_0 T}\right)_{ice} = -\frac{R}{\Delta H_{fus}} \ln a_w = -\beta_{ice} \ln a_w \tag{12}$$

where the ratio $\frac{R}{\Delta H_{fus}} = 0.001384 K^{-1}$, T_0 and T correspond to melting points of pure water and water + inhibitors, respectively. Therefore, the relation between suppression temperatures of water and hydrate is described as follows:

$$\frac{\left(\frac{\Delta T}{T_0 T}\right)_{hyd}}{\left(\frac{\Delta T}{T_0 T}\right)_{ice}} = \frac{-n\Delta H_{fus}}{-\Delta H_{hyd}} = \frac{\beta_{hyd}}{\beta_{ice}} \tag{13}$$

Knowledge of ice suppression point and beta ratio leads to the hydrate suppression temperature. This requires the awareness of ice suppression temperature before, which is not always known.

However, this data can be easily obtained in relation to hydrate suppression temperature measurement for HLS correlation.

5. Results and discussion

5.1. Pressure-Temperature diagrams of CP/CO_2 hydrate in the presence of salts.

In this section, there were nine experiment systems studied: NaCl-KCl 1.75wt%-1.75wt%, $MgCl_2$ 3.5wt%, $MgCl_2$ 5wt%, $MgCl_2$ 7wt%, $MgCl_2$ 10wt%, $CaCl_2$ 4wt%, $CaCl_2$ 5wt%, $CaCl_2$ 7wt%, $CaCl_2$ 10wt%. [74]. Initial conditions are drawn in **Table 2**. Then, results are compared with literature data with pure water (Zhang et al. [74]).

A **P**ressure-**T**emperature curve throughout an experiment is detailed and analyzed hereafter (see **Figure 2**). Each experiment was started at point **A** (the initial point, which is outside of the hydrate formation region). Then, the system was decreased down to approximately 1°C. A few hours later, hydrate formation starts at point **B**. Hydrate formation is an exothermic process, that led to the increase of temperature for a while on the diagram. After few days, the hydrate formation ended at point **C**. The liquid sample was taken here if possible. Then, the hydrate dissociation was performed by a stepwise increase in the system temperature until the dissociation curve meets the final equilibrium point **D**. At this point, there are four phases of CP-CO_2 clathrate hydrate (V-L_w-L_{HC}-H). This point is also called the "total dissociation point" and represents thermodynamic equilibrium. The other equilibrium points, after hydrate formation and during the dissociation process (before point D), are not necessarily thermodynamic equilibrium points, as discussed before (Maghsoodloo Babakhani et al. [45]). They are likely metastable points, assuming the coexistence of several hydrate phases.

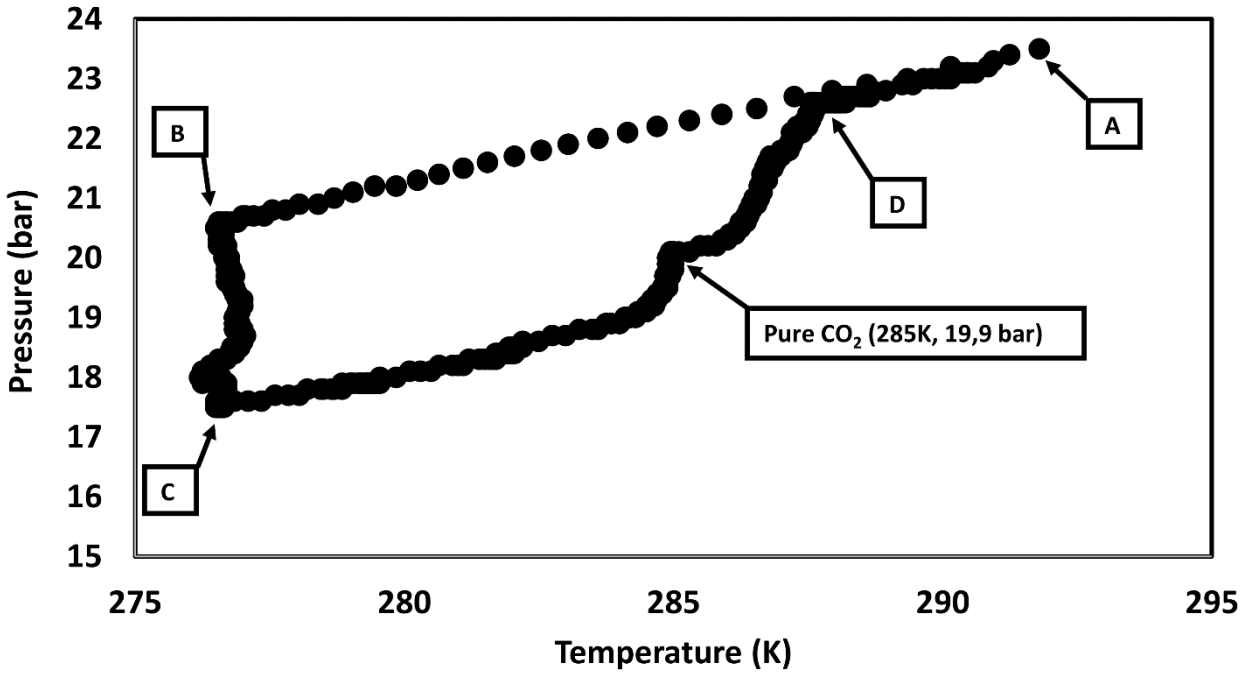

Figure 2. A P-T evolution of CP-CO_2 hydrate in the presence of $MgCl_2$ 7wt%.

Indeed, as mentioned by Maghsoodloo Babakhani et al., [45], our study provides further evidence for the probable existence of different types of hydrate structures in the system. Therefore, different phenomenon has appeared during the dissociation process. **Figure 2** illustrates one of the abnormal phenomena, observed in the present effort and comparable to the previous study which suggested decomposition of sI structure (likely pure CO_2 hydrates) at 19.9 bar and 285 K. This phenomenon has also appeared in the case of 10wt% $MgCl_2$ equimolar 1.75wt% of and NaCl-KCl as shown in Appendix A (Figures A1 and A2).

5.2. Experimental dissociation data

New four-phase equilibrium data for mixed CP-CO_2 hydrate in the presence of salts (NaCl-KCl, $MgCl_2$, and $CaCl_2$) at different concentrations are presented in **Table 5**. Water activities were calculated by PHREEQC. Activity coefficients were also determined. Supposed metastable points are represented i in supporting information.

From the final dissociation points in different cases, the final equilibrium curves of CP-CO_2 mixed hydrate in the presence of salts at different concentrations can be drawn (see **Figure 3**). The equilibrium curve of mixed CP-CO_2 in pure water was also plotted to compare the inhibition effect of salt on the hydrate formation. Erreur ! Source du renvoi introuvable. **3** presents that the results of this work agree adequately with the literature [38].

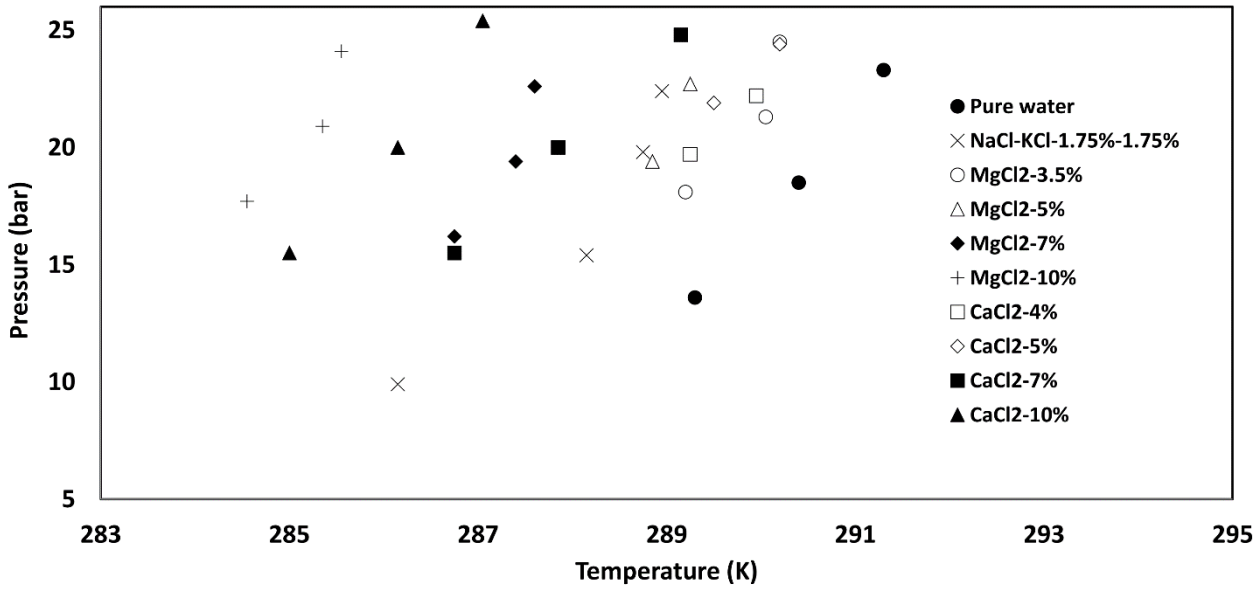

Figure 3. A typical P-T evolution of CP-CO_2 binary clathrate hydrate in the presence of salts of this work in comparison with pure water data of Zhang et al. [74].

Table 5. Experimental V-L_w-L_{HC}-H equilibrium data of mixed CP-CO_2 hydrate in the presence of salts (NaCl-KCl, $MgCl_2$, $CaCl_2$)

Solution concentrations wt%				P, (bar)	T, (K)	Water activity	Activity coefficient
NaCl	KCl	MgCl2	CaCl2				
±0.002wt%	±0.002wt%	±0.002wt%	±0.002wt%	±0.1 bar	±0.2K	±0.001	±0.001
1.75	1.75	0	0	22.4	289	0.979	0.991
1.75	1.75	0	0	19.8	288.8	0.981	0.992
1.75	1.75	0	0	15.4	288.2	0.980	0.991
1.75	1.75	0	0	9.9	286.2	0.980	0.991
0	0	3.5	0	19	290	0.981	0.988
0	0	3.5	0	18.1	289.2	0.980	0.987
0	0	3.5	0	21.3	290.1	0.981	0.988
0	0	3.5	0	24.5	290.2	0.980	0.987
0	0	5	0	22.7	289.3	0.970	0.980
0	0	5	0	19.4	288.9	0.971	0.981
0	0	7	0	22.6	287.6	0.953	0.956
0	0	7	0	19.4	287.4	0.955	0.969
0	0	7	0	16.2	286.8	0.955	0.969
0	0	10	0	24.1	285.6	0.927	0.947
0	0	10	0	20.9	285.4	0.928	0.948
0	0	10	0	17.7	284.6	0.926	0.946
0	0	0	4	22.2	289.95	0.982	0.989
0	0	0	4	19.7	289.3	0.982	0.989
0	0	0	5	24.4	290.2	0.977	0.985
0	0	0	5	21.9	289.5	0.977	0.985
0	0	0	7	15.5	289.2	0.964	0.976
0	0	0	7	20	287.9	0.963	0.976
0	0	0	7	24.8	286.8	0.964	0.976
0	0	0	10	25.4	287.1	0.939	0.957
0	0	0	10	20	286.2	0.938	0.956
0	0	0	10	15.5	285	0.941	0.959

These results offer compelling evidence for the inhibition characteristic of salt on the gas hydrates formation [2,41] as equilibrium curves shift to the left of the diagram with the increasing presence of salt. Hence, higher salt concentrations lead the system to harsher conditions to form a gas hydrate. Moreover, the inhibition of $MgCl_2$ is stronger than that of $CaCl_2$ at the same concentration.

5.3 Dissociation enthalpies and thermodynamic consistency

Taking advantage of the Clausius-Clapeyron equation [63] (**Eq. (2)),** we have calculated the molar dissociation enthalpies of CO_2-CP hydrates in presence of salts. **Figure 4** indicates that the molar enthalpy decreases with the increase of temperature and pressure (shown in **Figure B1** in Appendix B). According to **Table B1** in Appendix B it can be explained by a change of compressibility factor. We observed that with an increase of salt concentrations the molar dissociation enthalpy also has been decreased. The molar dissociation enthalpy change can vary between 140 and 162 kJ/mol for the presence of all salts, except $MgCl_2$-7% which remarkably excels others and strikes 211kJ/mol at 286.75 K. Since the increase of the absolute value of slope between ln(P) and 1/T increases the molar $\Delta_{\mathrm{diss}}H_{\mathrm{m}(CO_2)}$ (see **Figure B2** in Appendix B), the behavior of $MgCl_2$ can be explained by a very small difference in phase equilibrium temperatures compared (which is close to the temperature uncertainty) while the equilibrium pressure difference is about 4-5 bars at each four-phase equilibrium point. Because of that, the absolute value of the slope is higher than expected and hits the significant molar dissociation enthalpy.

Furthermore, we have calculated the molar dissociation enthalpies and compressibility factors of CO_2-CP hydrates in presence of other salts based on the literature data [45,60,74] and demonstrated them with corresponding phase equilibrium parameters in **Table B1** in Appendix B.

In **Table 6**, we have shown the thermodynamic consistency results for this work and Zhang et al. [74] (previously calculated by Maghsoodloo Babakhani et al. [45]).

Assessment 1: Generally speaking, assessment 1 for results of Zhang et al. [74] and Lee et al., [80] show overall satisfactory validation while this work fails in presence of 3.5%, 7% and 10% $MgCl_2$.

Assessment 2: Note that this assessment is based on the relative deviation of the slope, by considering $-\Delta_{\mathrm{diss}}H_{\mathrm{m}(CO_2)}/ZR$ relatively constant. According to Maghsoodloo Babakhani et al. [45] the results of Zhang et al. [74] and Lee et al., [80] have shown better results compared to this work, in terms of consistency to molar dissociation enthalpy. However, the main concern is the quality of the pressure vs temperature correlation for pure water equilibrium required for this test. Assessment 2 cannot be properly examined yet concerning CO_2/CP experiments, in our opinion.

Assessment 3: Last assessment has been provided as relative standard deviation, where the accurate calculation of T_0 is the key point of validation. As we have used T_0 only from Zhang et al. [74] for CO_2-CP hydrate, results sometimes acceptable and failed. Therefore, we should sound a note of caution with regard to such evaluation of results.

Table 6. Thermodynamic consistency assessment

		Assessment 1		Assessment 2		Assessment 3	
Salts	wt%	1-R^2 (%)	validation	$(A_{THI}-A_W)/A_W$ (%)	validation	% RSD	validation
Zhang et al. [74]							
NaCl	0	0.4	pass	NA	NA	NA	NA
	3.5	0.2	pass	-3.9	acceptable	22.4	fail
	7	0.1	pass	-3.8	acceptable	10.8	fail
	10	0.5	pass	7.9	fail	9.4	acceptable
	15	2.6	acceptable	-9.2	fail	3.6	pass
	25	2.8	acceptable	-1.2	pass	2.2	pass
Lee et al., 2019 [80]							
NaCl	3.5	2.6	pass	-6.4	fail	51.9	fail
	10	0.2	acceptable	-20.6	fail	5.9	acceptable
This work							
NaCl-KCl	1.75+1.75	3.3	acceptable	-3.63	acceptable	30.5	fail
$MgCl_2$	3.5	11	fail	-6.5	fail	21	fail
	5	0	pass	38	fail	12	fail
	7	6	fail	26	fail	11.3	fail
	10	8	fail	-4.4	acceptable	4.5	pass
$CaCl_2$	4	0	pass	-40	fail	5.8	acceptable
	5	0	pass	-45	fail	7.3	acceptable
	7	0.9	pass	-32	fail	4.7	pass
	10	0.3	pass	-17.4	fail	3.3	acceptable

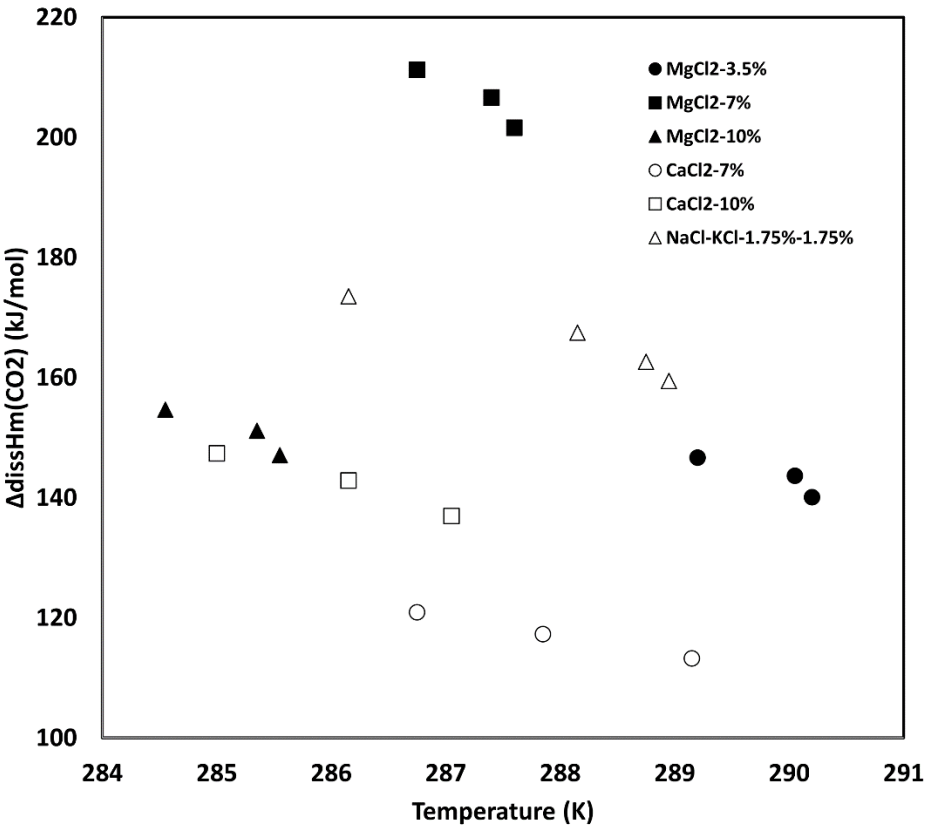

Figure 4. Dissociation enthalpy of CO_2-CP hydrate versus temperature (Since the error bars' size are smaller than the size of symbols in the figure, corresponding uncertainties for each point are shown in Table B1 in Appendix B)

5.4. Modelling results

5.4.1 vdW-P

The modeling results are shown in **Table 7**. Simulations present agreeable results compared to the experimental data. The minimum deviation is 0.05 K in the presence of 5 wt% $CaCl_2$. The modeling results for the final equilibrium point bring a positive perspective while the AAD is approximately 0.2K. This indicates that the equilibrium is well reproduced by using the optimized Kihara parameters for CP.

At some supposed metastable points, the deviations are quite high due to the heterogeneity of the system, as a result of the quick crystallization process [3]. The predicted and the experimental temperatures were closed to each other at the same pressure. They are plotted and compared clearly in **Figure 5**.

Table 7. Modeling results of final equilibrium points for mixed CP-CO_2 clathrate hydrate in the presence of salts.

Solution concentrations wt%				Experimental eq. conditions		vdW-P		HLS correlation		Ice melting point method	
NaCl	KCl	MgCl2	CaCl2	P, (bar)	T, (K)	Pred. T(K)	|Texp-Tpred|, K	Pred. T(K)	|Texp-Tpred|, K	Pred. T(K)	|Texp-Tpred|, K
±0.002wt%	±0.002wt%	±0.002wt%	±0.002wt%	±0.1 bar	±0.2K						
1.75	1.75	0	0	22.4	289.0	290.01	1.06	289.66	0.71	289.92	0.97
1.75	1.75	0	0	19.8	288.8	289.57	0.82	289.12	0.37	289.37	0.62
1.75	1.75	0	0	15.4	288.2	288.26	0.11	288.01	0.14	288.27	0.12
1.75	1.75	0	0	9.9	286.2	286.45	0.30	286.31	0.16	286.56	0.41
						AAD	**0.60**	**AAD**	**0.34**	**AAD**	**0.53**
0	0	3.5	0	18.1	289.2	288.87	0.33	288.14	1.06	288.46	0.74
0	0	3.5	0	21.3	290.1	289.57	0.49	288.92	1.13	289.24	0.81
0	0	3.5	0	24.5	290.2	290.32	0.12	289.44	0.76	289.77	0.43
						AAD	**0.31**	**AAD**	**0.98**	**AAD**	**0.66**
0	0	5	0	22.7	289.3	289.10	0.15	288.30	0.95	288.76	0.49
0	0	5	0	19.4	288.9	288.32	0.53	287.69	1.16	288.14	0.71
						AAD	**0.25**	**AAD**	**1.05**	**AAD**	**0.60**
0	0	7	0	22.6	287.6	287.74	0.14	287.01	0.59	287.59	0.01
0	0	7	0	19.4	287.4	287.14	0.26	286.48	0.92	287.04	0.36
0	0	7	0	16.2	286.8	286.32	0.43	285.71	1.04	286.27	0.48
						AAD	**0.25**	**AAD**	**0.85**	**AAD**	**0.28**
0	0	10	0	24.1	285.6	286.21	0.66	285.44	0.11	286.04	0.49
0	0	10	0	20.9	285.4	285.46	0.11	284.85	0.50	285.45	0.10
0	0	10	0	17.7	284.6	284.74	0.19	284.03	0.52	284.63	0.08
						AAD	**0.22**	**AAD**	**0.38**	**AAD**	**0.22**
0	0	0	4	19.7	289.3	290.06	0.81	288.60	0.65	288.54	0.71
0	0	0	4	22.2	290.0	289.56	0.39	289.13	0.82	289.06	0.89

						AAD	**0.21**	**AAD**	**0.73**	**AAD**	**0.80**
0	0	0	5	21.9	289.5	290.00	0.50	288.64	0.86	288.60	0.90
0	0	0	5	24.4	290.2	289.55	0.65	289.06	1.14	289.03	1.17
						AAD	**0.12**	**AAD**	**1.00**	**AAD**	**1.03**
0	0	0	7	15.5	286.8	286.99	0.24	286.00	0.75	286.09	0.66
0	0	0	7	20	287.9	288.01	0.16	287.04	0.81	287.13	0.72
0	0	0	7	24.8	289.2	289.02	0.13	288.03	1.12	288.12	1.03
						AAD	**0.18**	**AAD**	**0.89**	**AAD**	**0.80**
0	0	0	10	25.4	287.1	287.08	0.03	286.15	0.90	286.49	0.56
0	0	0	10	20	286.2	285.84	0.31	285.11	1.04	285.45	0.70
0	0	0	10	15.5	285.0	285.04	0.04	284.23	0.77	284.54	0.46
						AAD	**0.13**	**AAD**	**0.91**	**AAD**	**0.58**

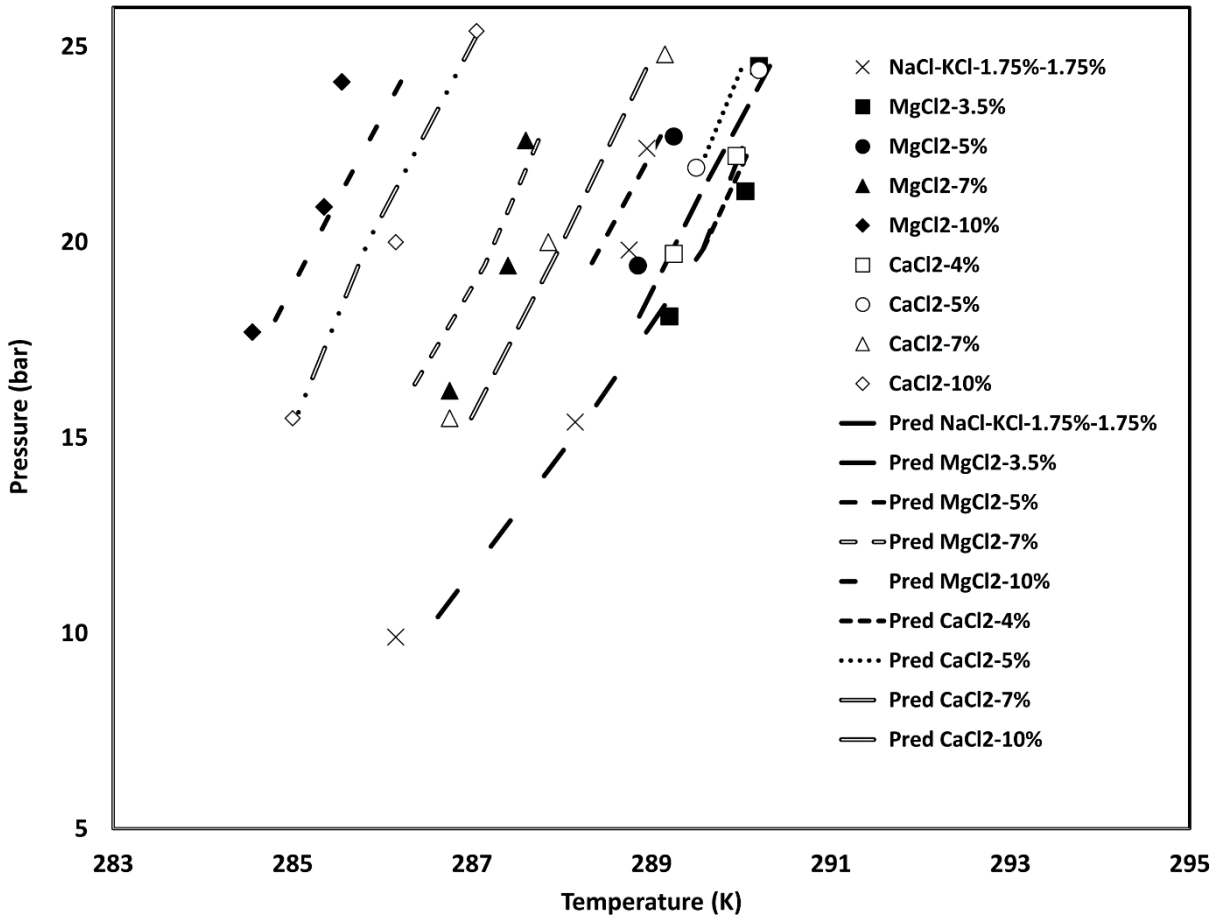

Figure 5. Measured and predicted (vdW-P approach) equilibrium data of binary CP/CO_2 hydrate in pure water and brine.

0

5.4.2 HLS correlation

According to the previous efforts of Hu et al. [69,78], as we have a system of mixed clathrates CP-CO_2 in presence of inhibitors, we decide to discuss each structure type separately.

Structure I. We remind that $\left(\frac{\Delta T}{T_0 T}\right)_1$ in Equation 8 belongs to structure I, which is the depression temperature of CO_2 hydrate system for pure water and in presence of inhibitors in case T_0 and T, respectively. Thus, it should be considered as the function of effective mole fraction X and calculated based on the fitting parameters ($C_1 = 0.0009377, C_2 = 0.00267$ and $C_3 = 0.03328$) of previous work of Hu et al. [78]. β_1 for structure I with CO_2 (0.0009186 K^{-1}) is taken from Hu et al. (method 1) [77].

Structure II. T_0 in $\left(\frac{\Delta T}{T_0 T}\right)_1$ is calculated based on the correlation of experimental data from the literature for pure CO_2-CP hydrate [45,49,74,79], shown in **Figure 6**. Beta β_2 of structure II for CO_2-CP is calculated based on the Eq. (6), where a_w is evaluated by 2 methods. The first is with help of correlation by Miyawaki et al. [81], as the function of effective mole fraction, to literature data of Maghsoodloo Babakhani et al. [45] and Zhang et al. [74] for pure CP-CO_2 hydrate and the second by the geochemical model PHREEQC. As a result, the calculated average β_2 are 0.000832 and 0.000853 by using each method, respectively. In our calculations, we have used β_2 as 0.000832.

The alpha is the ratio of betas, $\frac{\beta_2}{\beta_1} = \alpha$ was considered as constant and equal to 0.90592.

In **Table 7**, HLS correlation results of predicting equilibrium temperature show quite good results (AAD 0.34) for NaCl-KCl 1.75-1.75wt% and comparatively poor agreement for all concentrations of $MgCl_2$ and $CaCl_2$ with ADD 0.8-0.89K. Hence, there are several possible explanations for these results:

1. A correlation with R^2=0.967 for CO_2-CP hydrate (**Figure S3** in supporting information). There is a requirement for more accurate and reliable experimental data.
2. The beta β_2 for CP-CO_2 hydrate, which has been considered as constant for all equilibrium points at different salt concentrations. If there are a high variation in dissociation enthalpy of different salts throughout a concentration alteration, while the change of hydration number is negligible, we guess that the ratio $nR \,/\, \Delta_{\mathrm{diss}} H_{\mathrm{m}(CO_2)}$ could vary depending on salt and its concentration.

5.4.3 Ice melting point method (Sa and Sum proposition)

Since Sa and Sum [70] proposed an almost similar method as the aforementioned HLS correlation for mixed hydrates, it can thus be suggested to discuss only the suppression temperature of the water freezing point (Ice), because the suppression temperature of hydrate has been discussed previously in HLS modelling approach (structure II).

According to widely known phase equilibrium data for freshwater, T_0 equal to 273.15K (0°C). In the case of T, the presence of inhibitors (salts), we have done a literature review and correlate freezing point of solutions T as a function of weight fraction (wt%) for each salt. **Figures 6** and **7** present experimental data for $MgCl_2$ and $CaCl_2$ provided by Stephen et al. [82]. In the literature, there were very little data of freezing points for mixed NaCl-KCl solution. Therefore, based on the experimental data of Haghighi et al. [83], we have plotted curves (see **Figure 8**) for both of them, and since we work with comparatively low concentrations (1.75wt% for each salt, 3.5 wt% in total), it allowed us to get the average depression temperature equal to -1.85K.

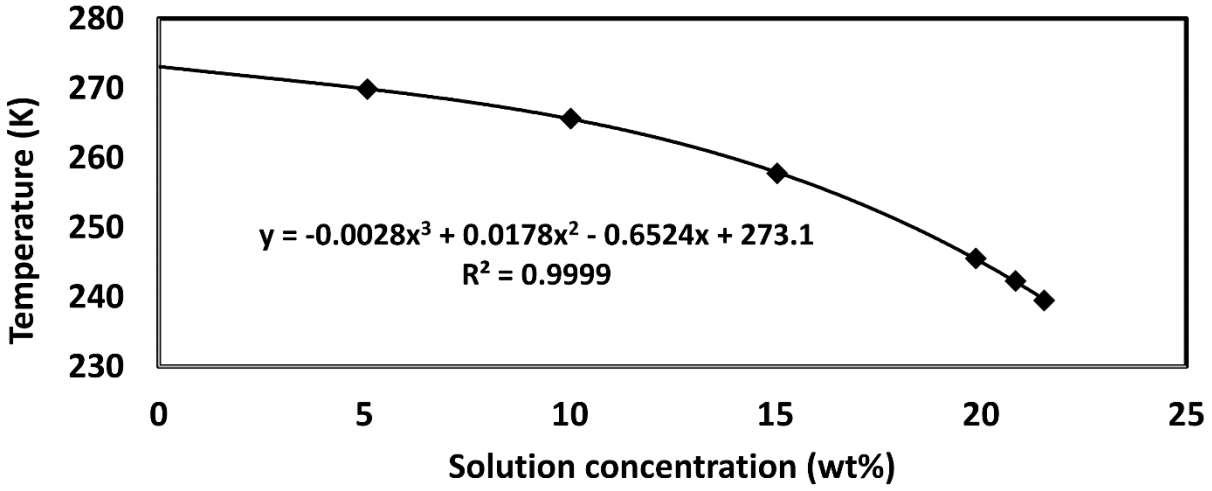

Figure 6. Phase diagram of $MgCl_2$ solution [82]

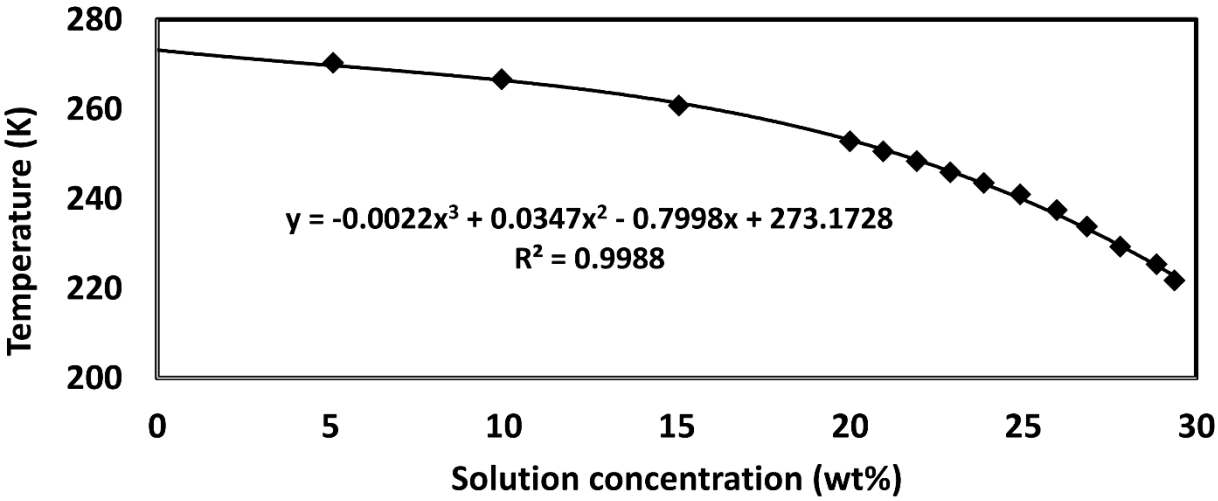

Figure 7. Phase diagram of $CaCl_2$ solution [82]

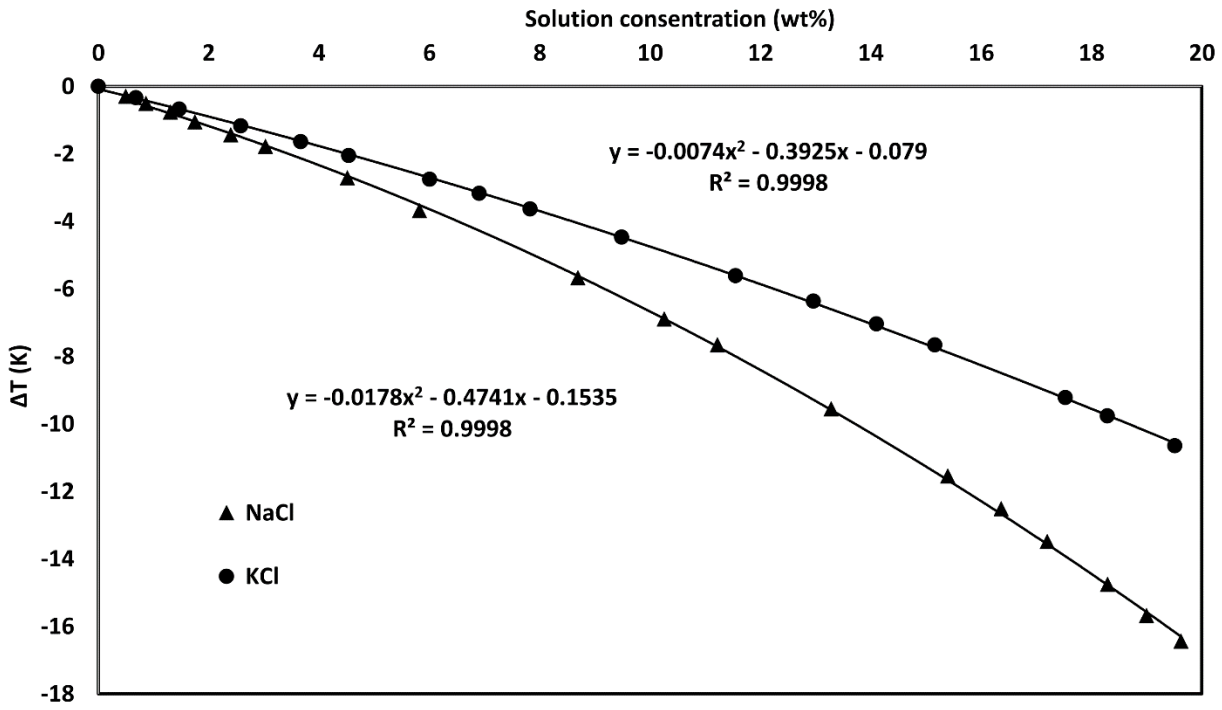

Figure 8. Phase diagram of NaCl and KCl solutions [83]

In **Table 7,** the ice melting point method showed a good agreement for NaCl-KCl and $MgCl_2$ with AAD less than 0.6K, but contrary to expectations validity of the method comparatively fails on the system in the presence of $CaCl_2$ with ADD 0.78 K. Other dissociation points can be found in supporting information **(Table S2)**.

Our work has led us to conclude that all three approaches can overall reproduce mixed CO_2-CP hydrate phase equilibrium temperatures. The average deviation between experimental and predicted among simulations has been constituted in **Table 8**.

Table 8. Average deviation (in K) of three models for predicting CO_2-CP hydrate in presence of salts

Models	NaCl-KCl	MgCl2	CaCl2
Number of exp. data points	4	11	10
vdW-P	0.57	0.26	0.16
HLS	0.34	0.80	0.89
Ice melting point method (HLS)	0.53	0.43	0.78

6. Conclusion

A new dataset for cyclopentane and carbon dioxide hydrates in presence of salts has been proposed. It includes new salts ($MgCl_2$ and $CaCl_2$), calculation of dissociation enthalpies, a thermodynamic consistency analysis, and new modelling approaches for such systems.

First new four-phase equilibrium data (V-L_w-L_{HC}-H) for CP-CO_2 binary hydrates in the presence of $MgCl_2$ and $CaCl_2$ was obtained. That is necessary for the development of hydrate-based desalination, or water treatment application. The results show the inhibition effect of salts on the formation of clathrate hydrates. Moreover, at the same concentration, the equilibrium curve of CP-CO_2 hydrate $MgCl_2$ solution is located on the left-hand side of that in $CaCl_2$ solution. That proves the inhibition property of Ca^{2+} is weaker than that of ion Mg^{2+}.

As observed previously, two crystallization phenomena have sometimes been observed. Accordingly, at least three dissociation behaviors have been witnessed during the dissociation processes. Consequently, different crystal structures could have been formed in the reactor. This could be a shred of evidence for the co-existence of sI simple CO_2 hydrate and sII binary CP-CO_2 hydrate.

Second, dissociation enthalpies have been calculated thanks to Clapeyron's equation and have been found comparable to literature data. Thermodynamic consistency has also been investigated and discussed in regard to encountered difficulties (some relevant data missing, and presence of liquid thermodynamic promoter).

Finally, modeling results using the van der Waals & Platteeuw model is acceptable to describe the equilibrium with the AAD is approximately 0.2 K compared to the experimental temperature.

HLS correlation and Sa et Sum approach based on ice freezing point also provide interesting results AAD < 0.89K and AAD < 0.78, respectively.

In perspective, the structures could be studied to determine the observations in this work by involving spectroscopic tools.

Acknowledgment

The authors would like to thank French National Research Agency (ANR) for financial support. Especially, this work is part of INNOHYD French ANR-18-CE05-0006 project.

The authors would also like to thank region Auvergne-Rhône-Alpes in France for financial support in the frame of SCUSI France-VietNam collaboration.

Finally, the authors would like to thanks Fabien Chauvy warmly, our laboratory technician who helped us so much.

CRediT authorship contribution statement

Angsar Serikkali: Investigation, writing –original draft, writing, review & editing. **Hieu Ngo Van**: Investigation, Writing –original draft. **Trung-Kien Pham**: Supervision. **Quang Duyen Le**: Supervision. **Jérôme Douzet**: Methodology. **Jean-Michel Herri**: Supervision. **Baptiste Bouillot**: Supervision, investigation, writing, review & editing.

Supplementary materials

Supplementary material associated with this article can be found, in the online version, at doi:10.1016/j.fluid.2022.113410 .

References

[1] C.A. Koh, E.D. Sloan, A.K. Sum, D.T. Wu, Fundamentals and Applications of Gas Hydrates, Annu. Rev. Chem. Biomol. Eng. (2011). https://doi.org/10.1146/annurev-chembioeng-061010-114152.

[2] E.D. Sloan, C.A. Koh, Clathrate Hydrates of Natural Gases, (2008).

[3] S. Maghsoodloo Babakhani, B. Bouillot, S. Ho-Van, J. Douzet, J.M. Herri, A review on hydrate composition and capability of thermodynamic modeling to predict hydrate pressure and composition, Fluid Phase Equilib. 472 (2018) 22–38. https://doi.org/10.1016/j.fluid.2018.05.007.

[4] S. Ho-van, J. Douzet, D. Le-quang, B. Bouillot, S. Ho-van, J. Douzet, D. Le-quang, B. Bouillot, J.H. Behavior, Behavior of cyclopentane hydrates formation and dissociation in pure water and in the presence of sodium chloride To cite this version : HAL Id : hal-01466636, (2017) 1–8.

[5] E.D. Sloan, Hydrocarbon Hydrate Flow Assurance History as a Guide to a Conceptual Model, Molecules. 26 (2021). https://doi.org/doi.org/10.3390/molecules26154476.

[6] H. Hashimoto, T. Yamaguchi, T. Kinoshita, Gas separation of fl ue gas by tetra- n -butylammonium bromide hydrates under moderate pressure conditions, Energy. 129 (2017) 292–298. https://doi.org/10.1016/j.energy.2017.04.074.

[7] S. Tomita, S. Akatsu, R. Ohmura, Experiments and thermodynamic simulations for continuous separation of CO 2 from CH 4 + CO 2 gas mixture utilizing hydrate formation, Appl. Energy. 146 (2015) 104–110. https://doi.org/10.1016/j.apenergy.2015.01.088.

[8] D. Saha, H.A. Grappe, A. Chakraborty, G. Orkoulas, Postextraction Separation, On-Board Storage, and Catalytic Conversion of Methane in Natural Gas: A Review, Chem. Rev. 116 (2016) 11436–11499. https://doi.org/10.1021/acs.chemrev.5b00745.

[9] W.T. LIBERSON, Functional electrotherapy., Trans. Am. Soc. Artif. Intern. Organs. 8 (1962) 373–377. https://doi.org/10.1097/00002480-196204000-00075.

[10] L.C. Tomé, I.M. Marrucho, Ionic liquid-based materials: A platform to design engineered CO2 separation membranes, Chem. Soc. Rev. 45 (2016) 2785–2824. https://doi.org/10.1039/c5cs00510h.

[11] J.R. Li, R.J. Kuppler, H.C. Zhou, Selective gas adsorption and separation in metal-organic frameworks, Chem. Soc. Rev. 38 (2009) 1477–1504. https://doi.org/10.1039/b802426j.

[12] S. Basu, A.L. Khan, A. Cano-Odena, C. Liu, I.F.J. Vankelecom, Membrane-based technologies for biogas separations, Chem. Soc. Rev. 39 (2010) 750–768. https://doi.org/10.1039/b817050a.

[13] W. Wang, C. Ma, P. Lin, L. Sun, A.I. Cooper, Gas storage in renewable bioclathrates, Energy Environ. Sci. 6 (2013) 105–107. https://doi.org/10.1039/c2ee23565j.

[14] K. Kim, H. Kang, Y. Kim, Risk assessment for natural gas hydrate carriers: A hazard identification (HAZID) study, Energies. 8 (2015) 3142–3164. https://doi.org/10.3390/en8043142.

[15] H. Ganji, J. Aalaie, S.H. Boroojerdi, A.R. Rod, Effect of polymer nanocomposites on methane hydrate stability and storage capacity, J. Pet. Sci. Eng. 112 (2013) 32–35. https://doi.org/10.1016/j.petrol.2013.11.026.

[16] S.M. Babakhani, A. Alamdari, Effect of maize starch on methane hydrate formation / dissociation rates and stability, J. Nat. Gas Sci. Eng. 26 (2015) 1–5. https://doi.org/10.1016/j.jngse.2015.05.026.

[17] R. Tarkowski, Underground hydrogen storage: Characteristics and prospects, Renew. Sustain. Energy Rev. 105 (2019) 86–94. https://doi.org/10.1016/j.rser.2019.01.051.

[18] K. Sordakis, C. Tang, L.K. Vogt, H. Junge, P.J. Dyson, M. Beller, G. Laurenczy, Homogeneous Catalysis for Sustainable Hydrogen Storage in Formic Acid and Alcohols, Chem. Rev. 118 (2018) 372–433. https://doi.org/10.1021/acs.chemrev.7b00182.

[19] L.J. Murray, M. Dinc, J.R. Long, Hydrogen storage in metal-organic frameworks, Chem. Soc. Rev. 38 (2009) 1294–1314. https://doi.org/10.1039/b802256a.

[20] P. Di Profio, S. Arca, F. Rossi, M. Filipponi, Comparison of hydrogen hydrates with existing hydrogen storage technologies: Energetic and economic evaluations, Int. J. Hydrogen Energy. 34 (2009) 9173–9180. https://doi.org/10.1016/j.ijhydene.2009.09.056.

[21] J. Andersson, S. Grönkvist, Large-scale storage of hydrogen, Int. J. Hydrogen Energy. 44 (2019) 11901–11919. https://doi.org/10.1016/j.ijhydene.2019.03.063.

[22] S. Oya, M. Aifaa, R. Ohmura, International Journal of Greenhouse Gas Control Formation , growth and sintering of CO 2 hydrate crystals in liquid water with continuous CO 2 supply : Implication for subsurface CO 2 sequestration, Int. J. Greenh. Gas Control. 63 (2017) 386–391. https://doi.org/10.1016/j.ijggc.2017.06.007.

[23] B. Prah, R. Yun, CO2 hydrate slurry transportation in carbon capture and storage, Appl. Therm. Eng. (2017). https://doi.org/10.1016/j.applthermaleng.2017.09.053.

[24] A. Hassanpouryouzband, J. Yang, B. Tohidi, E. Chuvilin, V. Istomin, B. Bukhanov, A. Cheremisin, CO2 Capture by Injection of Flue Gas or CO2-N2 Mixtures into Hydrate Reservoirs: Dependence of CO2 Capture Efficiency on Gas Hydrate Reservoir Conditions, Environ. Sci. Technol. 52 (2018) 4324–4330. https://doi.org/10.1021/acs.est.7b05784.

[25] A. Hassanpouryouzband, J. Yang, B. Tohidi, E. Chuvilin, V. Istomin, B. Bukhanov, A. Cheremisin, Insights into CO2 Capture by Flue Gas Hydrate Formation: Gas Composition Evolution in Systems Containing Gas Hydrates and Gas Mixtures at Stable Pressures, ACS Sustain. Chem. Eng. 6 (2018) 5732–5736. https://doi.org/10.1021/acssuschemeng.8b00409.

[26] B. Chazallon, C. Pirim, Selectivity and CO2 capture efficiency in CO2-N2 clathrate hydrates investigated by in-situ Raman spectroscopy, Chem. Eng. J. 342 (2018) 171–183.

https://doi.org/10.1016/j.cej.2018.01.116.

[27] F. Sun, Y. Yao, G. Li, X. Li, Geothermal energy development by circulating CO2 in a U-shaped closed loop geothermal system, Energy Convers. Manag. 174 (2018) 971–982. https://doi.org/10.1016/j.enconman.2018.08.094.

[28] F. Sun, Y. Yao, G. Li, X. Li, Geothermal energy extraction in CO2 rich basin using abandoned horizontal wells, Energy. 158 (2018) 760–773. https://doi.org/10.1016/j.energy.2018.06.084.

[29] F. Sun, Y. Yao, G. Li, X. Li, Performance of geothermal energy extraction in a horizontal well by using CO2 as the working fluid, Energy Convers. Manag. 171 (2018) 1529–1539. https://doi.org/10.1016/j.enconman.2018.06.092.

[30] H. Hashemi, S. Babaee, A.H. Mohammadi, P. Naidoo, D. Ramjugernath, Experimental study and modeling of the kinetics of refrigerant hydrate formation, J. Chem. Thermodyn. 82 (2015) 47–52. https://doi.org/10.1016/j.jct.2014.10.017.

[31] T. Ogawa, T. Ito, K. Watanabe, K. ichi Tahara, R. Hiraoka, J. ichi Ochiai, R. Ohmura, Y.H. Mori, Development of a novel hydrate-based refrigeration system: A preliminary overview, Appl. Therm. Eng. 26 (2006) 2157–2167. https://doi.org/10.1016/j.applthermaleng.2006.04.003.

[32] Z. Yin, J. Zheng, H. Kim, Y. Seo, P. Linga, Hydrates for cold energy storage and transport: A review, Adv. Appl. Energy. 2 (2021) 100022. https://doi.org/10.1016/j.adapen.2021.100022.

[33] X. Wang, M. Dennis, L. Hou, Clathrate hydrate technology for cold storage in air conditioning systems, Renew. Sustain. Energy Rev. 36 (2014) 34–51. https://doi.org/10.1016/j.rser.2014.04.032.

[34] P. Zhang, Z.W. Ma, An overview of fundamental studies and applications of phase change material slurries to secondary loop refrigeration and air conditioning systems, Renew. Sustain. Energy Rev. 16 (2012) 5021–5058. https://doi.org/10.1016/j.rser.2012.03.059.

[35] Y.F. Makogon, Natural gas hydrates - A promising source of energy, J. Nat. Gas Sci. Eng. 2 (2010) 49–59. https://doi.org/10.1016/j.jngse.2009.12.004.

[36] K.A. Kvenvolden, Methane hydrate a major reservoir of carbon in the shallow geosphere?, Chem. Geol. 71 (1988) 41–51.

[37] A. Hassanpouryouzband, E. Joonaki, M. Vasheghani Farahani, S. Takeya, C. Ruppel, J. Yang, N.J. English, J.M. Schicks, K. Edlmann, H. Mehrabian, Z.M. Aman, B. Tohidi, Gas hydrates in sustainable chemistry, Chem. Soc. Rev. 49 (2020) 5225–5309. https://doi.org/10.1039/c8cs00989a.

[38] M.S. Khan, B. Lal, K.M. Sabil, I. Ahmed, Desalination of seawater through gas hydrate process: An overview, J. Adv. Res. Fluid Mech. Therm. Sci. 55 (2019) 65–73.

[39] H.M.E. H.T. El-Dessouky, Fundamentals of Salt Water Desalination, 2002.

[40] IPCC, IPCC report Global Warming of 1.5 C: Summary for Policymakers, 2018.

[41] S. Ho-Van, B. Bouillot, J. Douzet, S.M. Babakhani, J.M. Herri, Cyclopentane hydrates-A candidate for desalination?, J. Environ. Chem. Eng. 7 (2019) 103359. https://doi.org/10.1016/j.jece.2019.103359.

[42] J.N. Zheng, M. Yang, B. Chen, Y. Song, D. Wang, Research on the CO2 Gas Uptake of Different Hydrate Structures with Cyclopentane or Methyl-cyclopentane as Co-guest Molecules, Energy Procedia. 105 (2017) 4133–4139. https://doi.org/10.1016/j.egypro.2017.03.877.

[43] S. Ho-Van, B. Bouillot, J. Douzet, S.M. Babakhani, J.M. Herri, Implementing Cyclopentane Hydrates Phase Equilibrium Data and Simulations in Brine Solutions, Ind. Eng. Chem. Res. 57 (2018) 14774–14783. https://doi.org/10.1021/acs.iecr.8b02796.

[44] S. Ho-Van, B. Bouillot, J. Douzet, S. Maghsoodloo, J.-M.M. Herri, S.M. Babakhani, J.-M.M. Herri, Experimental measurement and thermodynamic modeling of cyclopentane hydrates with NaCl, KCl, CaCl2, or NaCl-KCl present, Am. Inst. Chem. Eng. J. (2018). https://doi.org/10.1002/aic.16067.

[45] S. Maghsoodloo Babakhani, S. Ho-van, B. Bouillot, J. Douzet, J.M. Herri, S.M. Babakhani, S. Ho-van, B. Bouillot, J. Douzet, S.M. Babakhani, S. Ho-van, B. Bouillot, J. Douzet, Phase equilibrium measurements and modelling of mixed cyclopentane and carbon dioxide hydrates in presence of salts, Chem. Eng. Sci. 214 (2020) 115442. https://doi.org/10.1016/j.ces.2019.115442.

[46] S. Hong, S. Moon, Y. Lee, S. Lee, Y. Park, Investigation of thermodynamic and kinetic effects of cyclopentane derivatives on CO2 hydrates for potential application to seawater desalination, Chem. Eng. J. 363 (2019) 99–106. https://doi.org/10.1016/j.cej.2019.01.108.

[47] J. nan Zheng, M. Yang, Experimental investigation on novel desalination system via gas hydrate, Desalination. 478 (2020) 114284. https://doi.org/10.1016/j.desal.2019.114284.

[48] M. Karamoddin, F. Varaminian, Water desalination using R141b gas hydrate formation, Desalin. Water Treat. 52 (2014) 2450–2456. https://doi.org/10.1080/19443994.2013.798840.

[49] P.J. Herslund, K. Thomsen, J. Abildskov, N. von Solms, A. Galfré, P. Brântuas, M. Kwaterski, J.M. Herri, Thermodynamic promotion of carbon dioxide-clathrate hydrate formation by tetrahydrofuran, cyclopentane and their mixtures, Int. J. Greenh. Gas Control. 17 (2013) 397–410. https://doi.org/10.1016/j.ijggc.2013.05.022.

[50] S. Sun, X. Peng, Y. Zhang, J. Zhao, Y. Kong, Stochastic nature of nucleation and growth kinetics of THF hydrate, J. Chem. Thermodyn. (2016). https://doi.org/10.1016/j.jct.2016.12.026.

[51] W. Liu, S. Wang, M. Yang, Y. Song, S. Wang, J. Zhao, Investigation of the induction time for THF hydrate formation in porous media, J. Nat. Gas Sci. Eng. 24 (2015) 357–364. https://doi.org/10.1016/j.jngse.2015.03.030.

[52] H. Najibi, K. Momeni, M.T. Sadeghi, Theoretical and experimental study of phase equilibrium of semi-clathrate hydrates of methane + tetra-n-butyl-ammonium bromide aqueous solution, J. Nat. Gas Sci. Eng. (2015). https://doi.org/10.1016/j.jngse.2015.11.002.

[53] S. Han, Y.W. Rhee, S.P. Kang, Investigation of salt removal using cyclopentane hydrate formation and washing treatment for seawater desalination, Desalination. 404 (2017) 132–137. https://doi.org/10.1016/j.desal.2016.11.016.

[54] P.T. Ngema, P. Naidoo, A.H. Mohammadi, D. Ramjugernath, Phase stability conditions for clathrate hydrate formation in (fluorinated refrigerant + water + single and mixed electrolytes + cyclopentane) systems: Experimental measurements and thermodynamic modelling, J. Chem. Thermodyn. 136 (2019) 59–76. https://doi.org/10.1016/j.jct.2019.04.012.

[55] N.A. Sami, K. Das, J.S. Sangwai, N. Balasubramanian, Phase equilibria of methane and carbon dioxide clathrate hydrates in the presence of (methanol + MgCl2) and (ethylene glycol + MgCl 2) aqueous solutions, J. Chem. Thermodyn. 65 (2013) 198–203. https://doi.org/10.1016/j.jct.2013.05.050.

[56] A. Galfré, M. Kwaterski, P. Braîntuas, A. Cameirao, J.M. Herri, Clathrate hydrate equilibrium data for the gas mixture of carbon dioxide and nitrogen in the presence of an emulsion of cyclopentane in water, J. Chem. Eng. Data. (2014). https://doi.org/10.1021/je4002587.

[57] J. nan Zheng, M. jun Yang, Y. Liu, D. yong Wang, Y. chen Song, Effects of cyclopentane on CO2 hydrate formation and dissociation as a co-guest molecule for desalination, J. Chem. Thermodyn. (2017). https://doi.org/10.1016/j.jct.2016.09.006.

[58] J. Lee, K.S. Kim, Y. Seo, Thermodynamic, structural, and kinetic studies of cyclopentane + CO2 hydrates: Applications for desalination and CO2 capture, Chem. Eng. J. 375 (2019) 121974. https://doi.org/10.1016/j.cej.2019.121974.

[59] J.H. Sa, Y. Hu, A.K. Sum, Assessing thermodynamic consistency of gas hydrates phase equilibrium data for inhibited systems, Fluid Phase Equilib. 473 (2018) 294–299. https://doi.org/10.1016/j.fluid.2018.06.012.

[60] Z.Y. Chen, Q.P. Li, Z.Y. Yan, K.F. Yan, Z.Y. Zeng, X. Sen Li, Phase equilibrium and dissociation enthalpies for cyclopentane + methane hydrates in NaCl aqueous solutions, J. Chem. Eng. Data. 55 (2010) 4444–4449. https://doi.org/10.1021/je100597e.

[61] S. Ho-Van, B. Bouillot, J. Douzet, S.M. Babakhani, J.M. Herri, Experimental measurement and thermodynamic modeling of cyclopentane hydrates with NaCl, KCl, CaCl 2 , or NaCl-KCl present, AIChE J. 64 (2018) 2207–2218. https://doi.org/10.1002/aic.16067.

[62] D. Dalmazzone, L.P. Sales Silva, A. Delahaye, L. Fournaison, Calorimetric Characterization of Clathrate and Semiclathrate Hydrates, Gas Hydrates 1. (2017) 145–176. https://doi.org/10.1002/9781119332688.ch4.

[63] G.K. Anderson, Enthalpy of dissociation and hydration number of carbon dioxide hydrate from the Clapeyron equation, J. Chem. Thermodyn. 35 (2003) 1171–1183. https://doi.org/10.1016/S0021-9614(03)00093-4.

[64] S. Alavi, R. Ohmura, Understanding decomposition and encapsulation energies of structure I and II clathrate hydrates, J. Chem. Phys. 145 (2016). https://doi.org/10.1063/1.4964673.

[65] Y. Hu, B.R. Lee, A.K. Sum, Insight into increased stability of methane hydrates at high pressure from phase equilibrium data and molecular structure, Fluid Phase Equilib. 450 (2017) 24–29. https://doi.org/10.1016/j.fluid.2017.07.003.

[66] I.N. Tsimpanogiannis, V.K. Michalis, I.G. Economou, Enthalpy of dissociation of methane hydrates at a wide pressure and temperature range, Fluid Phase Equilib. 489 (2019) 30–40. https://doi.org/10.1016/j.fluid.2019.01.024.

[67] Z. Nasri, H. Binous, Applications of the Soave-Redlich-Kwong equation of state using mathematica®, J. Chem. Eng. Japan. 40 (2007) 534–538. https://doi.org/10.1252/jcej.40.534.

[68] J.H. van der Waals, J.C. Platteeuw, Clathrate Solutions, I (2007) 1–57. https://doi.org/10.1002/9780470143483.ch1.

[69] Y. Hu, B.R. Lee, A.K. Sum, Universal correlation for gas hydrates suppression temperature of inhibited systems: II. Mixed salts and structure type, AIChE J. 64 (2018) 2240–2250. https://doi.org/10.1002/aic.16116.

[70] J.H. Sa, A.K. Sum, Universal correlation for gas hydrates suppression temperature of inhibited systems: IV. Water activity, AIChE J. 67 (2021). https://doi.org/10.1002/aic.17293.

[71] J.-M. Herri, A. Bouchemoua, M. Kwaterski, A. Fezoua, Y. Ouabbas, A. Cameirao, Gas hydrate equilibria for CO2–N2 and CO2–CH4 gas mixtures—Experimental studies and thermodynamic modelling, Fluid Phase Equilib. 301 (2011) 171–190. https://doi.org/10.1016/j.fluid.2010.09.041.

[72] D. Le Quang, D. Le Quang, B. Bouillot, J.M. Herri, P. Glenat, P. Duchet-Suchaux, Experimental procedure and results to measure the composition of gas hydrate, during crystallization and at equilibrium, from N2-CO2-CH4-C2H6-C3H8-C4H10gas mixtures, Fluid Phase Equilib. (2016). https://doi.org/10.1016/j.fluid.2015.10.022.

[73] M. Wang, Z.G. Sun, C.H. Li, A.J. Zhang, J. Li, C.M. Li, H.F. Huang, Equilibrium Hydrate Dissociation Conditions of CO2+ HCFC141b or Cyclopentane, J. Chem. Eng. Data. 61 (2016) 3250–3253. https://doi.org/10.1021/acs.jced.6b00333.

[74] Y. Zhang, S.M. Sheng, X.D. Shen, X.B. Zhou, W.Z. Wu, X.P. Wu, D.Q. Liang, Phase Equilibrium of Cyclopentane + Carbon Dioxide Binary Hydrates in Aqueous Sodium Chloride Solutions, J. Chem. Eng. Data. 62 (2017) 2461–2465. https://doi.org/10.1021/acs.jced.7b00404.

[75] A. Galfré, Captage du dioxyde de carbone par cristallisation de clathrate hydrate en présence de cyclopentane : Etude thermodynamique et cinétique, Ecole Nationale Supérieure des Mines de Saint-Etienne, 2014.

[76] B. Bouillot, J.M. Herri, Framework for clathrate hydrate flash calculations and implications on the crystal structure and final equilibrium of mixed hydrates, Fluid Phase Equilib. 413 (2016) 184–195. https://doi.org/10.1016/j.fluid.2015.10.023.

[77] Y. Hu, J.H. Sa, B.R. Lee, A.K. Sum, Universal correlation for gas hydrates suppression temperature of inhibited systems: III. salts and organic inhibitors, AIChE J. 64 (2018) 4097–4109. https://doi.org/10.1002/aic.16369.

[78] Y. Hu, B.R. Lee, A.K. Sum, Universal correlation for gas hydrates suppression temperature of inhibited systems: I. Single salts, AIChE J. 63 (2017) 5111–5124. https://doi.org/10.1002/aic.15846.

[79] Y. Matsumoto, T. Makino, T. Sugahara, K. Ohgaki, Phase equilibrium relations for binary mixed hydrate systems composed of carbon dioxide and cyclopentane derivatives, Fluid Phase Equilib. (2014). https://doi.org/10.1016/j.fluid.2013.10.057.

[80] J. Lee, K.S. Kim, Y. Seo, Thermodynamic, structural, and kinetic studies of cyclopentane + CO2 hydrates: Applications for desalination and CO2 capture, Chem. Eng. J. 375 (2019) 121974. https://doi.org/10.1016/j.cej.2019.121974.

[81] O. Miyawaki, A. Saito, T. Matsuo, K. Nakamura, Activity and Activity Coefficient of Water in Aqueous Solutions and Their Relationships with Solution Structure Parameters, Biosci. Biotechnol. Biochem. 61 (1997) 466–469. https://doi.org/10.1271/bbb.61.466.

[82] E.J.F. Stephen A. Ketcham, L. David Minsk, Robert R. Blackburn, MANUAL OF PRACTICE FOR AN EFFECTIVE ANTI-ICING PROGRAM, Hanover, New Hampshire 03755-1290, 1996.

[83] H. Haghighi, A. Chapoy, B. Tohidi, Freezing point depression of electrolyte solutions: Experimental measurements and modeling using the cubic-plus-association equation of state, Ind. Eng. Chem. Res. 47 (2008) 3983–3989. https://doi.org/10.1021/ie800017e.

Appendix A: PT curves for other systems

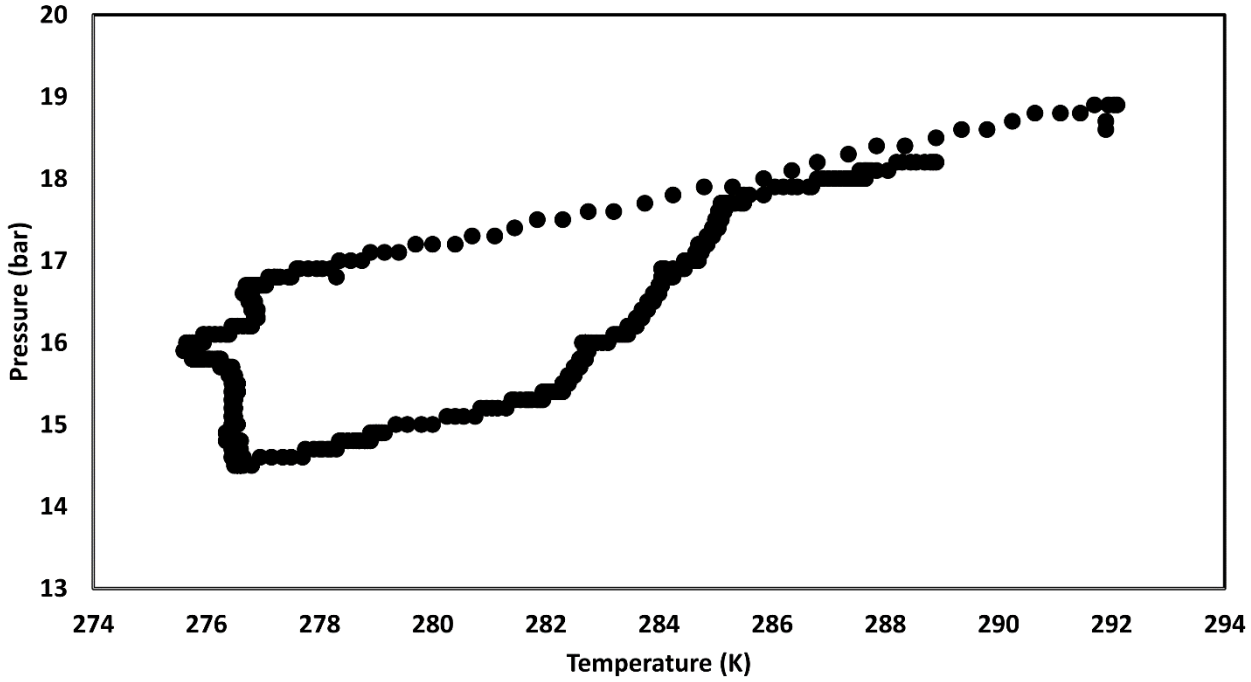

Figure A1. A P-T evolution of CP-CO_2 hydrate in the presence of $MgCl_2$ 10 wt%.

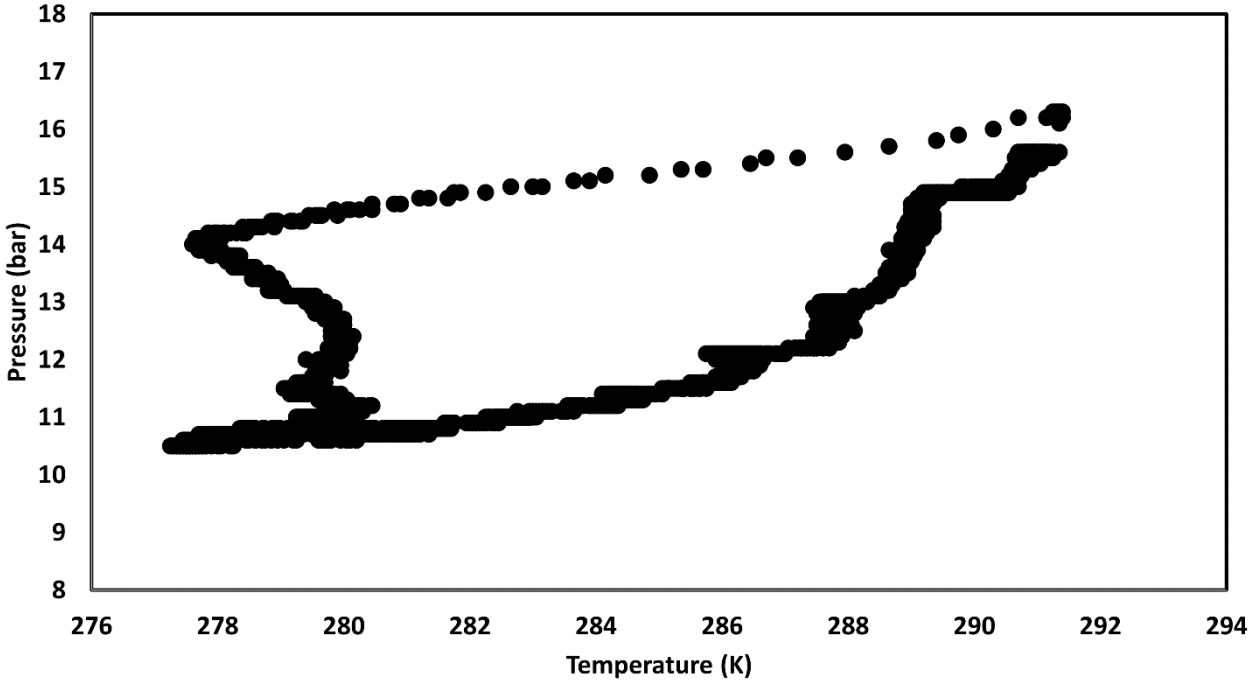

Figure A2. A P-T evolution of CP-CO_2 hydrate in the presence of NaCl-KCl 1.75-1.75 wt%.

Appendix B: Consistency and dissociation enthalpy

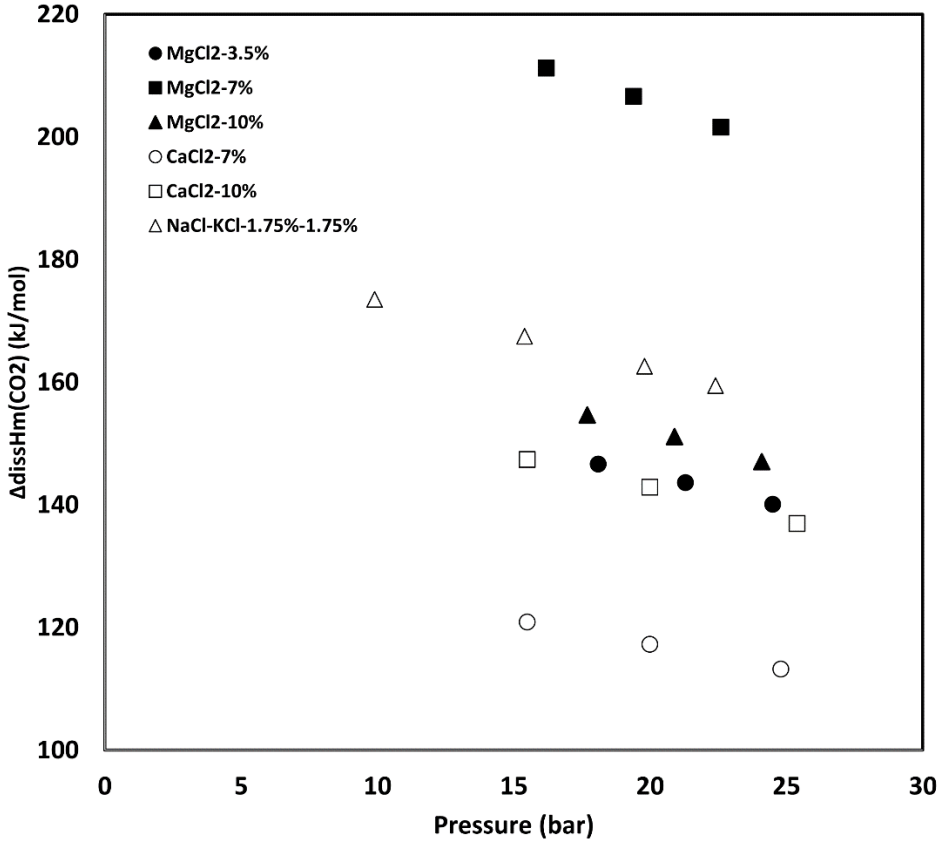

Figure B1. Dissociation enthalpy of CO_2-CP hydrate versus pressure

(Since the error bars' size are smaller than the size of symbols in the figure, the corresponding uncertainties for each point are shown in Table B1 in Appendix B)

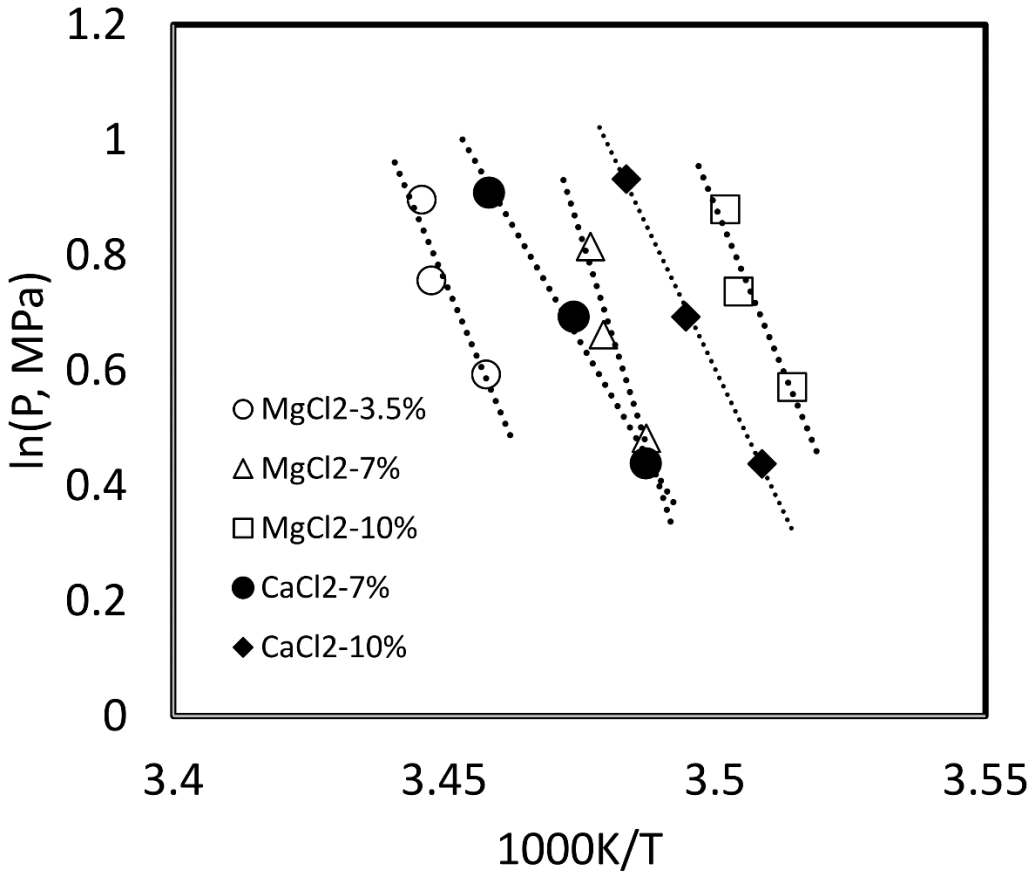

Figure B2. Natural logarithm of equilibrium pressure vs the reciprocal equilibrium temperature

(The error bars' size are smaller than the size of symbols in the figure)

Table B1. Four phase equilibrium conditions (T and P), compressibility factor (Z) and dissociation enthalpy (ΔH_{diss}) of mixed CO_2-CP hydrate in the presence of salts (wt%).

This work	wt%	T,K	P,bar	Z	ΔdissH	Abs. unc. ΔdissH, Kj/mol
	±0.002%	±0.2K	±0.1 bar			±
CO_2-CP-water-NaCl-KCl	1.75-1.75	288.95	22.4	0.865	149.32	0.34
	1.75-1.75	288.75	19.8	0.882	152.29	0.39
	1.75-1.75	288.15	15.4	0.909	156.87	0.51
	1.75-1.75	286.15	9.9	0.942	162.51	0.89
CO_2-CP-water-$MgCl_2$	3.5	289.2	18.1	0.894	146.63	0.38
	3.5	290.05	21.3	0.875	143.61	0.32
	3.5	290.2	24.5	0.854	140.05	0.28
	7	287.6	22.6	0.862	201.57	0.43
	7	287.4	19.4	0.883	206.60	0.50
	7	286.75	16.2	0.903	211.23	0.62
	10	285.55	24.1	0.847	147.04	0.29
	10	285.35	20.9	0.871	151.11	0.34
	10	284.55	17.7	0.891	154.63	0.41
CO_2-CP-water-$CaCl_2$	7	286.75	15.5	0.907	120.88	0.37
	7	287.85	20	0.880	117.23	0.28
	7	289.15	24.8	0.850	113.19	0.22
	10	287.05	25.4	0.841	136.94	0.26
	10	286.15	20	0.878	142.83	0.34
	10	285	15.5	0.905	147.36	0.45

Zhang et al. 2017	wt%	T,K	P,bar	Z	delta H	Abs. unc. ΔdissH, Kj/mol
	a	±0.1K	0.2 bar			±
CO_2-CP-water-NaCl	3.5	287.9	14.1	0.918	173.91	0.99
	3.5	289	18.7	0.891	168.82	0.67
	3.5	289.7	22.7	0.865	163.82	0.52
	3.5	290.3	26.5	0.841	159.26	0.42
	3.5	290.7	30.6	0.812	153.76	0.35
	7	286.2	14.2	0.915	173.91	0.98
	7	287.2	18.9	0.886	168.33	0.66
	7	288	23.1	0.859	163.19	0.51
	7	288.5	26.8	0.835	158.60	0.41
	7	288.9	30.2	0.810	153.84	0.35

	10	284.4	14	0.915	194.16	1.12
	10	285.3	17.9	0.891	189.14	0.80
	10	285.9	21.5	0.866	183.84	0.62
	10	286.4	25.8	0.837	177.70	0.49
	10	286.8	29.8	0.807	171.31	0.40
	15	281.1	14.8	0.905	158.34	0.85
	15	282	18.8	0.879	153.76	0.61
	15	282.6	21.1	0.863	150.94	0.52
	15	283.1	24.3	0.841	147.05	0.43
	15	283.3	28.1	0.811	141.81	0.35
	25	269.8	11.8	0.915	173.61	1.26
	25	270.8	15	0.891	169.09	0.89
	25	271.4	18.2	0.865	164.25	0.68
	25	271.8	21.3	0.840	159.50	0.55
	25	272	24.5	0.811	153.97	0.45
Maghsoodloo Babakhani et al. 2020	wt%	T,K	P,bar	Z	delta H	Abs. unc. ΔdissH, Kj/mol
	±0.002%	±0.2K	±0.1 bar			±
CO_2-CP-water-NaCl	7	288.35	23.7	0.855	141.18	0.29
	7	287.25	18.8	0.887	146.32	0.37
	7	285.3	11.4	0.932	153.79	0.66
CO_2-CP-water-KCl	3.5	291.8	33.2	0.795	126.11	0.19
	3.5	291.75	33	0.797	126.32	0.20
	3.5	290.7	24.4	0.855	135.57	0.27
	3.5	289.85	18.2	0.894	141.71	0.37
	3.5	287.6	10.9	0.937	148.50	0.67
	3.5	284.75	6.6	0.960	152.22	1.33
	7	289.7	31.7	0.801	136.77	0.22
	7	288.85	24.7	0.850	145.15	0.28
	7	287.4	17.5	0.895	152.93	0.41
	7	286.45	13.5	0.920	157.22	0.56
	7	284.8	9.3	0.944	161.34	0.89
CO_2-CP-water-NaCl-KCl	1,75-1,75	291.2	34.7	0.782	132.80	0.20
	1,75-1,75	290.35	27.9	0.830	140.89	0.25
	1,75-1,75	289.65	23.5	0.859	145.86	0.30
	1,75-1,75	288.45	16.3	0.904	153.50	0.44
	1,75-1,75	286.45	9.9	0.942	159.89	0.82

	1,75-1,75	284.55	6.9	0.958	162.70	1.34
Chen et al. 2010	wt%	T,K	P,bar	Z	delta H	Abs. unc. ΔdissH, Kj/mol
	a	a	a			
CH_4-CP-water-NaCl	0	286.67	4.8	0.991	130.95	a
	0	289.35	7.9	0.985	130.24	a
	0	292.26	15.25	0.973	128.59	a
	0	295.75	27.6	0.954	126.08	a
	0	300.02	56.94	0.916	121.04	a
	0	301.31	71.51	0.900	119.02	a
	3.5	284.5	6.22	0.988	121.46	a
	3.5	286.71	8.25	0.984	121.02	a
	3.5	289.24	13.5	0.975	119.88	a
	3.5	291.95	22.5	0.960	118.06	a
	3.5	295.77	42.69	0.930	114.42	a
	3.5	297.73	59.06	0.910	111.91	a
	3.5	299.06	74	0.894	109.96	a
	3.5	301.31	105.13	0.871	107.11	a
	3.5	303.28	150.94	0.858	105.56	a
	7	284.4	7.88	0.984	113.54	a
	7	286.57	11.83	0.977	112.71	a
	7	289.14	17.75	0.967	111.54	a
	7	292.01	27	0.951	109.75	a
	7	295.67	49.56	0.921	106.26	a
	7	297.94	71.13	0.894	103.16	a
	7	299.33	88	0.880	101.53	a
	7	301.31	118.88	0.880	101.53	a
	7	303.28	178.06	0.862	99.47	a
	10	284.4	11	0.978	107.52	a
	10	286.57	16.19	0.968	106.46	a
	10	289.14	22.19	0.959	105.37	a
	10	292.01	33.44	0.940	103.34	a
	10	295.67	57.88	0.908	99.83	a
	10	297.94	83.13	0.882	96.94	a
	10	299.33	104.81	0.866	95.23	a
	10	300.71	142.61	0.855	93.97	a
	10	301.31	163.44	0.856	94.12	a

[a] absolute uncertainties were not provided by author

Appendix C: Evaluation of the errors (õ) on the calculation of the molar dissociation enthalpy

According to Clausius-Clapeyron equation [63]:

$$\frac{d\ln(P)}{d(1/T)} = \frac{-\Delta_{\text{diss}}H_{\text{m}(CO_2)}}{ZR} \tag{2}$$

In a first approximation, we can write that

$$\frac{\tilde{o}[\Delta_{\text{diss}}H_{\text{m}(CO_2)}]^2}{\Delta_{\text{diss}}H_{\text{m}(CO_2)}{}^2} = \frac{\tilde{o}[\Delta_{\text{diss}}H_{\text{m}(CO_2)}]^2}{(ZR)^2 \times lnP^2 \times T^2} \tag{14}$$

$$\frac{\tilde{o}[\Delta_{\text{diss}}H_{\text{m}(CO_2)}]^2}{(ZR)^2 \times lnP^2 \times T^2} = \frac{(ZR)^2[\frac{T^2 * \tilde{o}[P]^2}{P^2} + lnP^2 \times \tilde{o}[T]^2]}{(ZR)^2 \times LnP^2 \times T^2} \tag{15}$$

so we can give an evaluation:

$$\frac{\tilde{o}[\Delta_{\text{diss}}H_{\text{m}(CO_2)}]^2}{\Delta_{\text{diss}}H_{\text{m}(CO_2)}{}^2} = \frac{\tilde{o}[P]^2}{lnP^2 \times P^2} + \frac{\tilde{o}[T]^2}{T^2} + \frac{\tilde{o}[Z]^2}{Z^2} \tag{16}$$

Since the errors are mainly due to the accuracy in the estimation of pressure and temperature:

$$\frac{\tilde{o}[\Delta_{\text{diss}}H_{\text{m}(CO_2)}]^2}{\Delta_{\text{diss}}H_{\text{m}(CO_2)}{}^2} \approx \frac{\tilde{o}[P]^2}{lnP^2 \times P^2} + \frac{\tilde{o}[T]^2}{T^2} \tag{17}$$

$$\tilde{o}[\Delta_{\text{diss}}H_{\text{m}(CO_2)}] \approx \sqrt{\frac{\tilde{o}[P]^2}{lnP^2 \times P^2} + \frac{\tilde{o}[T]^2}{T^2}} \tag{18}$$

and

$$\tilde{o}[lnP] = \sqrt{\frac{\tilde{o}[P]^2}{lnP^2 \times P^2}} \tag{19}$$

$$\tilde{o}[T] = \sqrt{\frac{\tilde{o}[T]^2}{T^2}} \tag{20}$$

Note that:

-the error on evaluation of the pressure is õ(P)=0.1 bar

-the error on evaluation of the temperature is õ(T)=0.2 K

-the error on the evaluation of compressibility factor is considered as negligible